Geochemistry Geophysics Geosystems G3
AN ELECTRONIC JOURNAL OF THE EARTH SCIENCES
Published by AGU and the Geochemical Society

Technical Brief
Volume 8, Number 3
24 March 2007
Q03014, doi:10.1029/2006GC001455
ISSN: 1525-2027

Click Here for Full Article

A user-friendly one-dimensional model for wet volcanic plumes

Larry G. Mastin
U. S. Geological Survey, Cascades Volcano Observatory, 1300 SE Cardinal Court, Building 10, Suite 100, Vancouver, Washington 98683, USA (lgmastin@usgs.gov)

[1] This paper presents a user-friendly graphically based numerical model of one-dimensional steady state homogeneous volcanic plumes that calculates and plots profiles of upward velocity, plume density, radius, temperature, and other parameters as a function of height. The model considers effects of water condensation and ice formation on plume dynamics as well as the effect of water added to the plume at the vent. Atmospheric conditions may be specified through input parameters of constant lapse rates and relative humidity, or by loading profiles of actual atmospheric soundings. To illustrate the utility of the model, we compare calculations with field-based estimates of plume height (~9 km) and eruption rate (>~4×10^5 kg/s) during a brief tephra eruption at Mount St. Helens on 8 March 2005. Results show that the atmospheric conditions on that day boosted plume height by 1–3 km over that in a standard dry atmosphere. Although the eruption temperature was unknown, model calculations most closely match the observations for a temperature that is below magmatic but above 100°C.

Components: 11,466 words, 14 figures, 5 tables.

Keywords: volcanic plumes; volcanic ash; eruption modeling.

Index Terms: 8428 Volcanology: Explosive volcanism; 8409 Volcanology: Atmospheric effects (0370); 8488 Volcanology: Volcanic hazards and risks.

Received 22 August 2006; **Revised** 4 December 2006; **Accepted** 15 January 2007; **Published** 24 March 2007.

Mastin, L. G. (2007), A user-friendly one-dimensional model for wet volcanic plumes, *Geochem. Geophys. Geosyst.*, *8*, Q03014, doi:10.1029/2006GC001455.

1. Introduction

[2] During a pyroclastic eruption, a volcanic jet shoots out of an eruptive vent at several tens to more than 150 meters per second, driven by expanding gas. The jet is initially denser than the surrounding atmosphere and begins to decelerate through negative buoyancy and turbulent interaction with surrounding air. Along jet margins these processes generate cauliflower-like vortices that entrain air and heat it, reducing the bulk density of the entire jet, in many cases, to less than that of the surrounding atmosphere. Once it becomes buoyant, such a jet develops into a plinian or subplinian plume, rising kilometers to tens of kilometers until its heat is diluted enough that buoyancy is lost. Jets that lose their momentum before becoming buoyant collapse back onto the Earth's surface and transform into pyroclastic flows, surges and ignimbrites.

[3] The factors that affect plume rise and collapse can be dominated by the presence of water and the thermodynamics of condensation and evaporation. Liquid water can become entrained in pyroclastic jets

This paper is not subject to U.S. copyright.
Published in 2007 by the American Geophysical Union.

during some Surtseyan eruptions [*Thorarinsson*, 1967]; water and steam at boiling-point temperatures can drive phreatic and hydrothermal eruptions [*Mastin*, 1995]; and entrainment of water-saturated air can turn buoyant volcanic plumes into ash-laden thunderheads.

[4] The basic physics behind the ascent and collapse of volcanic columns has been understood for nearly half a century [*Morton et al.*, 1956a; *Settle*, 1978; *Wilson et al.*, 1978]. Within the past two decades the effects of magma type and vent conditions [*Woods*, 1988; *Woods and Bower*, 1995]; atmospheric conditions [*Sparks et al.*, 1997; *Woods*, 1993]; external surface water [*Koyaguchi and Woods*, 1996], thermal disequilibrium, and particle fallout [*Woods and Bursik*, 1991] have been assessed in increasing detail through numerical calculations.

[5] Despite its apparent complexity, a steady 1-D plume model can run on standard desktop computers, hence exploration of the factors that affect volcanic plume height or collapse need not be limited to investigators who develop these models. In this paper I present a user-friendly one-dimensional, steady volcanic plume model that considers atmospheric condensation, ice formation, and energetics of added external water. The model ("Plumeria") is intended for students, researchers, and educators, is freely downloadable as an executable file (http://vulcan.wr.usgs.gov/Projects/Mastin or GERM Web site) and runs on Microsoft (use of trade names does not imply endorsement of these products) Windows® -based computers through a graphical user interface (Figure 1; instructions are provided in Appendix A). The model's utility is illustrated in a sample application to a brief tephra eruption at Mount St. Helens, Washington. For brevity, the constitutive relations and assumptions are summarized here; full equations and solution procedures are detailed in Appendix B.

2. Conservation Equations

[6] Plumeria computes plume properties by dividing the plume into a series of control volumes (Figure 2) having horizontal upper and lower boundaries and thickness dz. Within each control volume the flux in mass (M), momentum (Mu) and energy (E) are conserved by equating the vertical gradient in these properties to lateral inputs from entrained air, using the formulation given by *Woods* [1988, 1993]. Following this formulation, the plume is divided into a momentum-dominated gas-thrust region immediately above the vent, and an overlying buoyancy-dominated convective region. Effects of particle fallout and thermal disequilibrium are ignored. In both regions the inward velocity u^{amb} of entrained air is assumed to be a constant fraction ε of plume velocity u, based on the observed linear rate of widening of laboratory plumes in similar fluids (e.g., air plumes in air or water plumes in water) [*Batchelor*, 1954; *Morton et al.*, 1956b] (see *Turner* [1973] for a discussion). Within the gas-thrust region the entrainment rate is adjusted by the factor $\sqrt{\rho/\rho^{amb}}$ [*Woods*, 1988] to account for density differences between the jet and ambient fluid, following results of *Thring and Newby* [1953] and *Hinze* [1975]. In the near-vent region, effects of vent geometry, pressure waves and jet inhomogeneity on entrainment are all ignored. These considerations lead to the following conservation equations:

Mass

Gas-thrust region

$$\frac{dM}{dz} = \frac{d(\pi r^2 \rho u)}{dz} = 2\pi r \varepsilon u \sqrt{\rho \rho^{amb}} \tag{1}$$

Convective region

$$\frac{dM}{dz} = \frac{d(\pi r^2 \rho u)}{dz} = 2\pi r \rho^{amb} \varepsilon u \tag{2}$$

Momentum

$$\frac{d(Mu)}{dz} = \pi r^2 \left(\rho^{amb} - \rho\right) g \tag{3}$$

Energy

$$\frac{dE}{dz} = \frac{d}{dz}\left[M\left(\frac{u^2}{2} + gZ + h\right)\right] = \left(gZ + h^{amb}\right)\frac{dM}{dz} \tag{4}$$

where r is the plume radius; ρ and ρ^{amb} are the densities of the jet and the ambient atmosphere, respectively, g is gravitational acceleration, Z is the height of the center of the control volume above the vent, and h and h^{amb} are the enthalpies per unit mass of the plume mixture and of the ambient atmosphere, respectively. The entrainment rate ε is assumed constant with a value of 0.09 [*Woods*, 1988, 1993]. Values of ρ^{amb} and h^{amb} are calculated assuming ideal gas relations (Appendix B).

[7] Following *Woods* [1988], the gas thrust region is assumed to extend to an elevation at which the plume density is less than that of the ambient atmosphere (*Glaze and Baloga* [1996] use a slightly different formula in which entrainment rate is continuous between these regions). The momentum

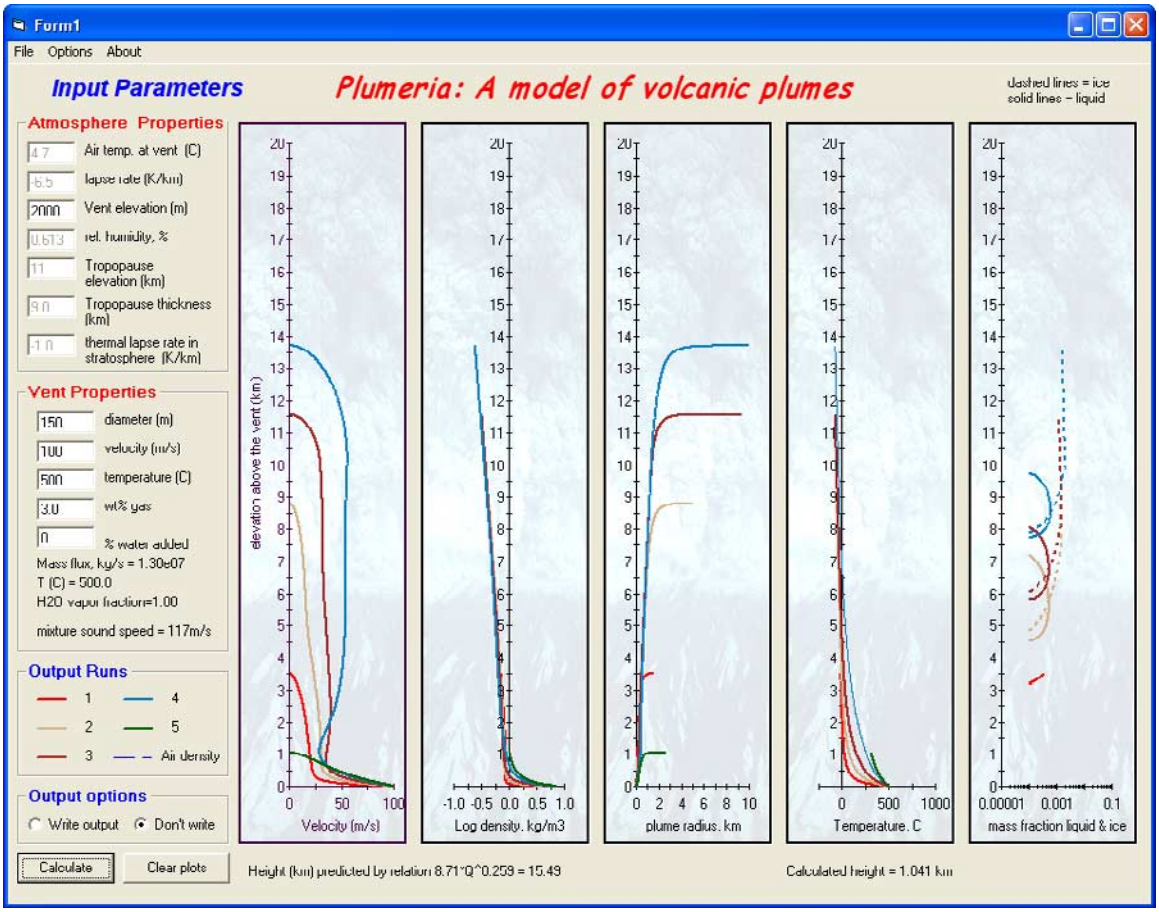

Figure 1. Graphical user interface of Plumeria.

equation assumes that the plume ascent is driven by the density difference between the plume and the ambient atmosphere. The energy equation assumes that no work or heat is transferred into or out of the control volume other than that advected by the plume itself and by entrained air.

[8] Equations (1) through (4) are numerically integrated from the vent upward until the vertical velocity drops below 0.1 m/s. At each step, velocity u and enthalpy h are obtained by combining integrated terms (e.g., $u = Mu/M$; $h = E/M - u^2/2 - gZ$). The density, temperature (T), and mass fraction of pyroclasts, air, and water in its various phases are computed assuming that these phases are homogeneously distributed, are in thermal equilibrium, and, at $T > 0°$C, that condensed liquid water is in chemical equilibrium with water vapor. I follow meteorological models [e.g., *Khairoutdinov and Randall*, 2003] in assuming that all condensed water is liquid at $T > -10°$, ice at $T < -40°$, and, at $T = -10°$ to $-40°$C, is a coexisting mixture of both phases with the relative proportions of each phase

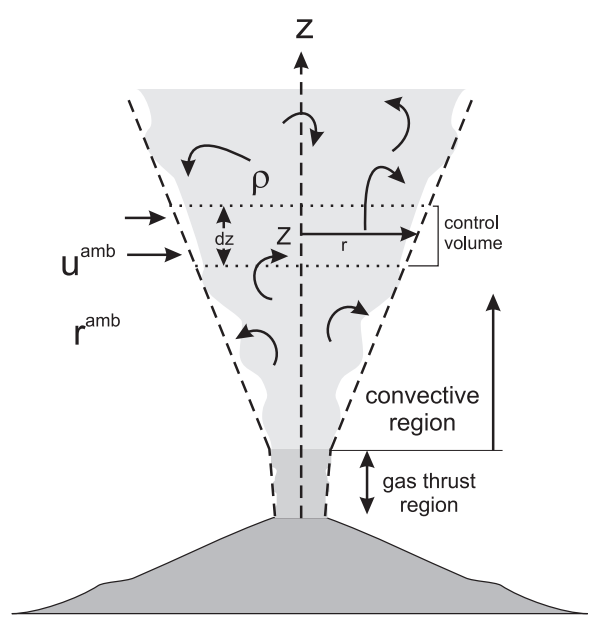

Figure 2. Illustration of the main parts of a volcanic plume.

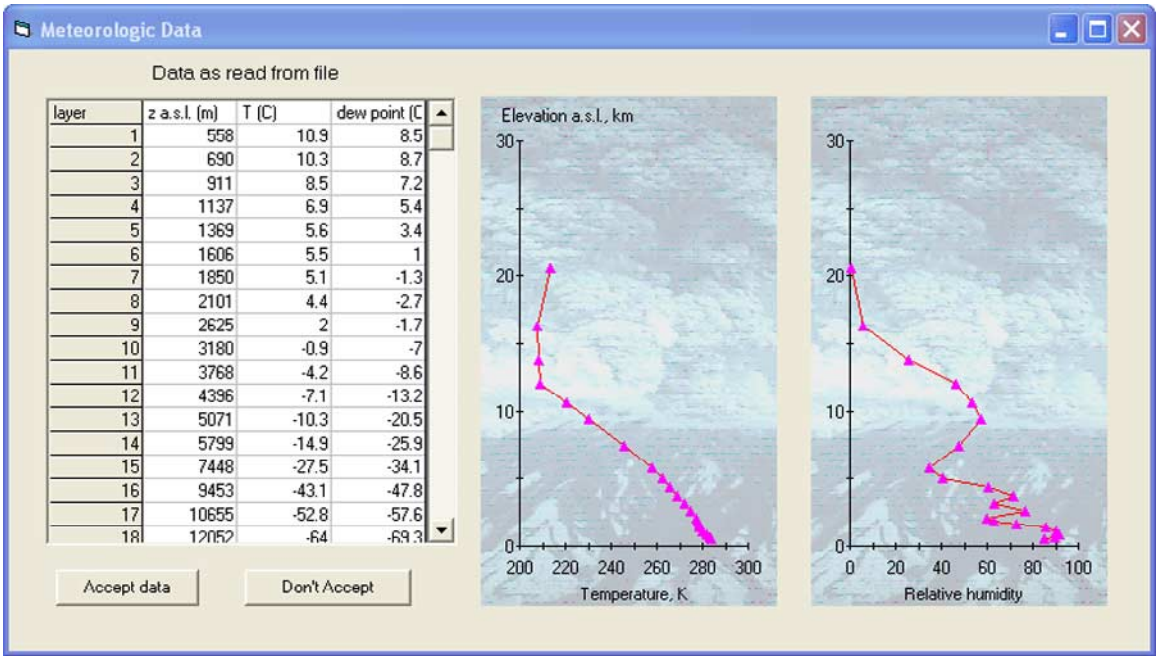

layer	z a.s.l. (m)	T (C)	dew point (C
1	558	10.9	8.5
2	690	10.3	8.7
3	911	8.5	7.2
4	1137	6.9	5.4
5	1369	5.6	3.4
6	1606	5.5	1
7	1850	5.1	-1.3
8	2101	4.4	-2.7
9	2625	2	-1.7
10	3180	-0.9	-7
11	3768	-4.2	-8.6
12	4396	-7.1	-13.2
13	5071	-10.3	-20.5
14	5799	-14.9	-25.9
15	7448	-27.5	-34.1
16	9453	-43.1	-47.8
17	10655	-52.8	-57.6
18	12052	-64	-69.3

Figure 3. Meteorological data dialog box, illustrating the atmospheric conditions at Mount St. Helens used in modeling the 8 March 2005 plume. This dialog box is used to import and plot meteorological data.

varying linearly with temperature. Solving for the temperature and the mass fractions of liquid water, water vapor, and ice at each step requires an iterative procedure of picking a temperature, calculating equilibrium phases at that temperature, summing their constituent enthalpies to obtain a total enthalpy, comparing that enthalpy with that

Figure 4. Photograph of the 8 March 2005 tephra eruption from Mount St. Helens, Washington (USA), taken from the SSW at approximately 5:45 PM (PST). Note that the plume is not anvil-shaped as is typical of strong plumes [*Bonadonna and Phillips*, 2003] but appears to bend over above the vent and rise more steeply a few kilometers downwind. The plume shape is partly related to temporal changes in eruption intensity, which, on the basis of seismic records, began to wane about ten minutes before this photo was taken. The plume shape may also result from particle fallout near the vent increasing the plume buoyancy. Particle fallout is not considered in the current plume model.

obtained by integrating (4), adjusting temperature, and recalculating until these two enthalpies agree.

3. Model Input

[9] Input parameters are entered in text boxes on the left-hand side of the user window (Figure 1). Specified vent properties include the vent diameter ($d_0 = 2r_0$), velocity (u_0), magma temperature (T_m), mass fraction of gas in the magma (n_0), and mass fraction external water (m_w^{ext}) added to the eruptive plume (see Appendix A for important caveats on adjusting these parameters). The fluxes in mass ($\pi r_0^2 \rho u_0$), momentum ($\pi r_0^2 \rho u_0^2$), and energy ($\pi r_0^2 \rho u_0 (h + u_0^2/2)$) at the vent are calculated from these terms and from the mixture density (ρ) and enthalpy (h_{vent}), which are determined by combining the mass fractions, enthalpies, and densities of the various phases assuming the gas components to be ideal, the magmatic gas to consist entirely of H_2O, and the mixture to be at ambient atmospheric pressure (Appendix B). When external water is present, Plumeria calculates equilibrium mass fractions of liquid and vapor assuming that the mixture has thermally equilibrated at atmospheric pressure before rising out of the vent and that the enthalpy of the mixture does not change during equilibration.

[10] Input atmospheric properties include profiles of temperature and relative humidity (r_h), which can be specified in either of two ways: (1) by entering a troposphere thermal lapse rate (dT/dz), basal tropopause elevation, tropopause thickness, stratospheric thermal lapse rate, and constant relative humidity (r_h) into text boxes in the upper left part of the interface window (Figure 1), or (2) by opening a second window (Figure 3) that loads and plots ASCII data containing profiles of temperature and dew point temperature (T_D) obtained from soundings posted by the National Oceanic and Atmospheric Administration (http://www.arl.noaa.gov/ready/amet.html) (see Appendix A for specific instructions). These data are used to calculate ρ^{amb} and h^{amb} for use in (1) through (4).

[11] Equations (2)–(4) are integrated using a modified form of routine rkqs.f from *Press et al.* [1992], which employs a fifth-order Runge-Kutta scheme with automatic adjustment of step size. The integration is carried out from the vent to the elevation at which the upward velocity is less than 0.1 m/s. A comparison of Plumeria model output with that of published one-dimensional steady state model results [*Koyaguchi and Woods*, 1996; *Sparks et al.*, 1997; *Woods*, 1988, 1993] is presented in Appendix C. The Plumeria results generally compare well with published works; differences of up to 15% in, for example, plume height, are thought to result primarily from slightly different methods of calculating enthalpy and water saturation in the atmosphere.

4. Application: The 8 March 2005 Tephra Eruption of Mount St. Helens

[12] The utility of Plumeria can be illustrated in a study of a brief tephra-forming eruption that took place at Mount St. Helens, Washington (USA) on 8 March 2005 [*Houlié et al.*, 2005; *Scott et al.*, 2007]. The eruption began at 17:25 PST after about an hour and a half of gradually increasing seismicity [*Moran et al.*, 2007]. Aerial observers (C. D. Miller and J. Pallister, USGS, written communication, 2005) noted a continuous column fed by spurts at intervals of one to three minutes, sending a light-colored plume to several kilometers height within a few minutes (Figure 4). Commercial pilots estimated the maximum plume height to be about 11000 m above sea level (8900 m above the vent). A high level of seismicity continued until about 17:35, followed by somewhat lower seismicity that lasted until about 17:50, and low-level ash emission that continued well after 18:00 [*Moran et al.*, 2007]. During the following six hours, satellite images tracked the eruptive cloud as far east as western Montana (500 km eastward; Figure 5b).

[13] Tephra sampled along three traverses downwind of Mount St. Helens (Figure 5a) suggested an approximate volume within 5 km^2 of the vent of $\sim 5 \times 10^4$ m^3 (dense-rock equivalent, DRE); but trace amounts reported at least to Ellensburg, WA (150 km NE, Figure 5b), suggest a total areal coverage >5,000 km^2, and total volume greater than 10^5 m^3. Assuming that most of this material was expelled in the first ten minutes and particle density is $\sim$2500 kg/m^3, the mass flow rate during the vigorous phase probably exceeded about 4×10^5 kg/s.

[14] The facts surrounding this eruption make it difficult to categorize as either juvenile or phreatic. Blocks ejected during the event were distributed in a pattern that suggested a source vent on the north or northwest margin of the active lava dome (Figure 5a). Tephra is composed of crushed, nearly holocrystalline, poorly vesicular fragments that resemble fault gouge on the dome and conduit margin [*Pallister et al.*, 2005]. Thus an origin

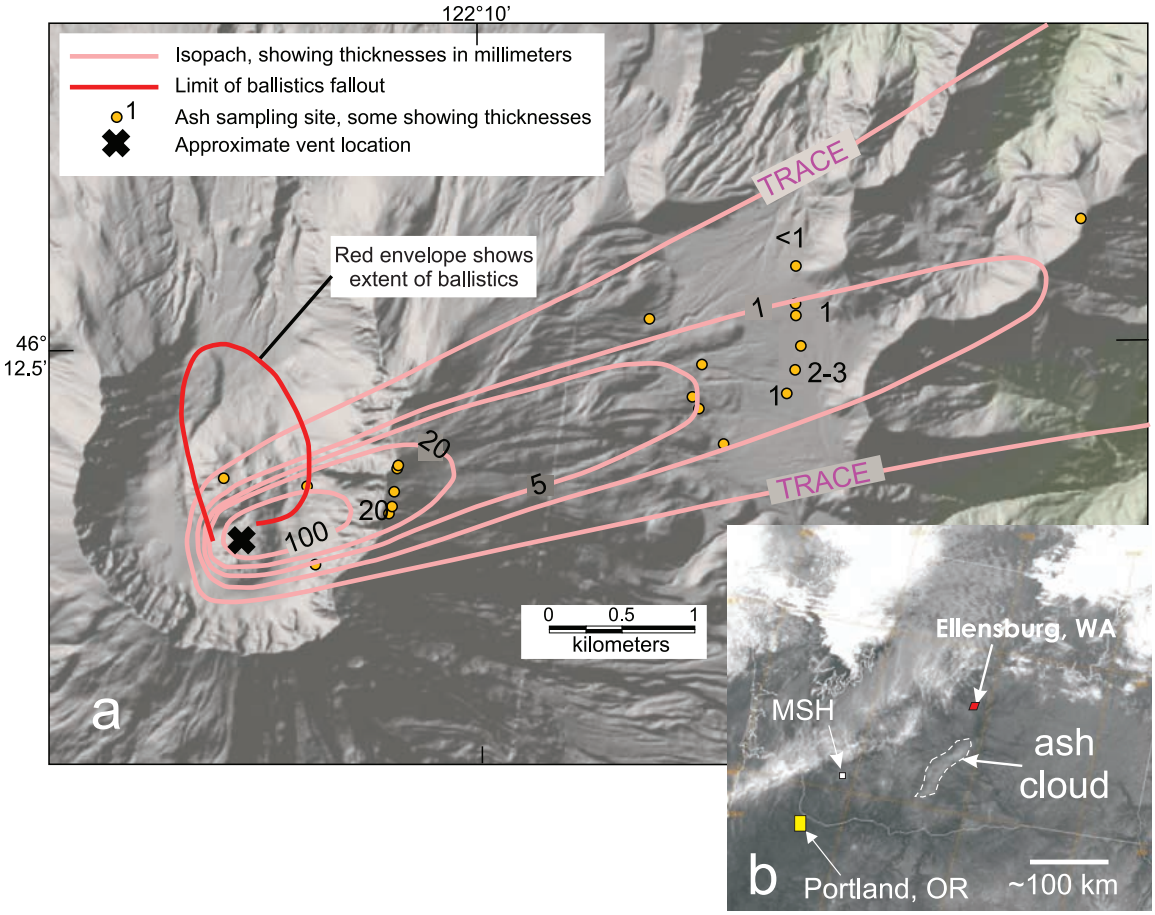

Figure 5. (a) Sampling localities of tephra from the 8 March 2005 eruption downwind from Mount St. Helens, along with very approximate isopach contours (purple) and the approximate limit of ballistic blocks during the eruption (red). Ash thicknesses are in millimeters. One additional traverse lies east of the mapped area. (b) Air Force Weather Agency visible satellite image of the eruptive cloud (outlined), taken at 7:45 PM PST. MSH, Mount St. Helens.

along the dome margin is deemed likely, with a driving fluid that could have been either magmatic gas, heated groundwater, or some combination of these. The high plume, however, suggests significant buoyancy, perhaps driven by magmatic heat. An important question was whether a plume of this height, with the mass flow rate inferred from the duration and minimum deposit volume, could have been generated by a steam-driven eruption.

[15] In order to address this question I calculate plume height for a range of mass eruption rate, eruptive temperature, and gas content; and compare the results with the observed height. The 20- to 40-minute eruption lasted several times longer than the time required for a plume to ascend 9 km (about 5 minutes as calculated by Plumeria). Thus it appears that this eruption can be reasonably modeled using a steady state model such as Plumeria. Atmospheric sounding data from above Mount St. Helens at the time of the eruption were downloaded from the NOAA Web site (http://www.arl.noaa.gov/ready/amet.html) and used as input atmospheric conditions (Figure 3). The plots in Figure 1 illustrate model results using an eruptive temperature of T = 500°C, a mass fraction of magmatic gas n_0 equal to 0.03 (a reasonable first guess), an ejection velocity u_0 of 100 m/s, no added water, and vent diameters of 10, 25, 50, 100, and 150 m for runs 1, 2, 3, 4, and 5, respectively. Each model run took 2–4 seconds to calculate and plot. In the final run (the dark green lines, run #5), the eruptive column collapsed after reaching about 1 km height. In runs 1 through 4, water can be seen to condense out of the plume starting at elevations of 3–8 km (solid lines on the

right-hand plot), and ice (dashed lines) begins to form at ~5–8 km height.

[16] A similar series of runs was then made for T = 100–900°C, n_0 = 0.02–0.35, and u_0 = 100 m/s. (Because the origin of the driving fluid is unknown, the term n_0 used here does not necessarily imply gas of magmatic origin but rather the amount of gas (as specified in the "wt% gas" text box) at the initial specified temperature.) For each run, the plume height (shown on the bottom right-hand side of the Figure 1 window) and the mass flux (shown in the "vent properties" box of Figure 1) were written into a spreadsheet and the results plotted as height versus mass eruption rate (Figure 6). External water was not explicitly added in these runs; rather, the eruption temperature and the mass fraction of magmatic gas were adjusted to represent a driving fluid that was cooler than magmatic. In the case where the eruption temperature equaled 100°C, the enthalpy was sufficient to vaporize all water in the plume at the vent.

[17] A one-dimensional steady state model such as Plumeria is ideally suited for strong plumes in which the ascent velocity is significantly greater than the horizontal wind velocity. Such plumes form vertical columns with anvil-shaped heads and a cloud of tephra extending downwind at the elevation of neutral buoyancy [*Bonadonna and Phillips*, 2003]. Easterly winds on 8 March at Mount St. Helens were about 15–20 m/s, comparable to the ascent velocity of the plume (Figure 1), and thus produced a plume that translated eastward with height (Figure 4). Following previous ash plume models [e.g., *Carey and Sparks*, 1986], I assume that the wind did not significantly affect plume height. This should be the case so long as most of the plume extended above the turbulent boundary layer created by topography and no layers of significant wind shear exist as represented by discontinuities in wind speed or direction. NOAA sounding data suggest that no such shears existed on this date.

[18] Results in Figure 6 illustrate several points. First, all of the plume heights calculated for the atmospheric conditions at Mount St. Helens on that day (blue lines) exceed those predicted (red lines) for a standard atmosphere [*United States Committee on Extension to the Standard Atmosphere*, 1976] having a sea level temperature of 0°C, a thermal lapse rate in the troposphere of 6.5°C/km, a troposphere thickness of 11 km, a 9-km-thick tropopause, and no atmospheric humidity. At a given mass flow rate the calculated plume heights also exceed that given (black dotted lines) by the empirical best-fit relation through compiled observations of plume height and eruption rate [*Sparks et al.*, 1997, p. 118]:

$$H = 1.67Q^{0.259} \tag{5}$$

where H is column height in kilometers and Q is the dense rock equivalent discharge rate in cubic meters per second (calculated from mass flow rate using a magma density of 2500 kg m^{-3}). The discrepancy is greatest for the blue curves, which use the local atmospheric conditions, though some discrepancy still exists for the red curves, which use a standard dry atmosphere.

[19] The blue curves exceed the height of the black empirical curves mostly because of atmospheric moisture and the small size of this eruption. Twenty-eight of the 31 plume-height observations on which (5) is based are larger than the 8 March event; and larger eruptions tend to be buoyed less by atmospheric moisture than small eruptions [*Sparks et al.*, 1997, Figure 4.11] (Appendix C, Figure C2). At T = 100°C, the height of the red curve exceeds the empirical curve height mostly due to the high gas content (n_0 = 0.25) used in the red-curve model runs. The greater height of the 900°C red curve in Figure 6d relative to the 500°C in Figure 6c reflects the effect of temperature on plume height, which is not considered in the empirical relation. At T = 900°C (Figure 6d) and n_0 = 0.03, the red curve lies above the empirical black dashed curve by 1 or 2 km, which is similar to the discrepancy between this curve and the *Woods* [1988] model [*Sparks et al.*, 1997, Figure 5.2] at this temperature and mass flow rate. At Plinian mass flow rates (~10^7 kg/s), Plumeria and the model of *Woods* [1988] roughly agree with the empirical relation at n_0 = 0.03 and T = 800–900°C.

[20] Figure 6a shows that, under the 8 March 2005 atmospheric conditions at Mount St. Helens, eruptions as cool as 100°C could generate plumes as high as the one observed (Figure 6a), but only when n_0 > ~0.25 and at significantly lower eruption rates than the minimum estimated (~4 × 10^5 kg/s; red vertical dotted line). At T = ~900°C, the observed plume height can be reached with n_0 = 0.02–0.03, but the mass eruption rate required to generate the observed height is less than the inferred minimum value (Figure 6d). Eruption temperatures of roughly 500°C (Figure 6c) generate the observed plume height at mass eruption rates that are above the estimated minimum value.

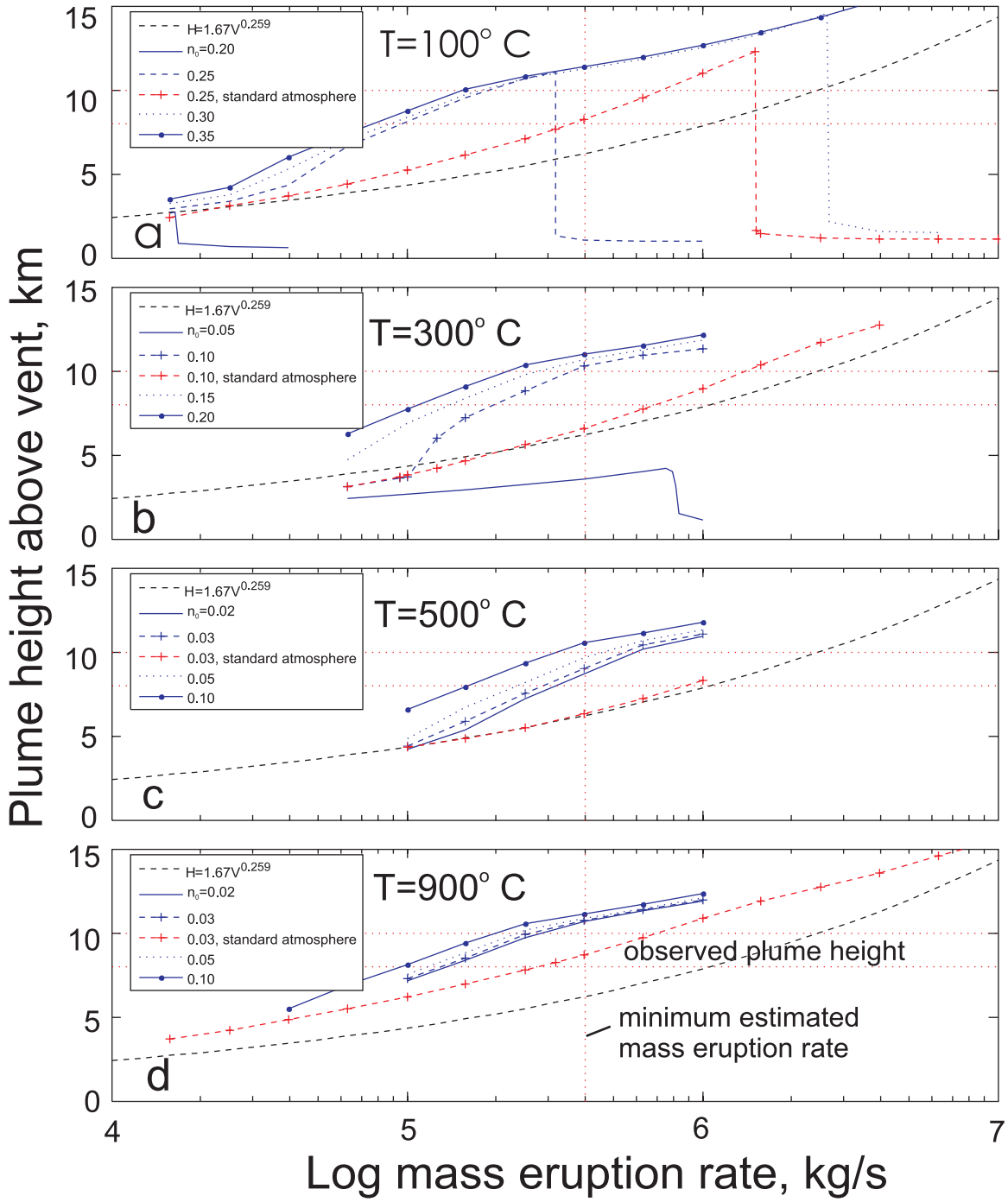

Figure 6. Calculated plume height using eruption temperatures of 100–900°C, n_0 = 0.015–0.35, and an ejection velocity of 100 m/s. Model results are compared with the empirical relation $H = 1.67V^{0.259}$ [*Sparks et al.*, 1997, p. 118], where the plume height (H) is in kilometers and V is the volumetric flow rate of magma (DRE) in m^3/s. Also shown (red dotted lines with crosses) are model results in a dry standard atmosphere [*United States Committee on Extension to the Standard Atmosphere*, 1976]. Horizontal red dotted lines denote the observed plume height (8900 m above the vent) with an uncertainty of plus or minus 1 km.

[21] These results are consistent with the possibility, already suggested by the geologic circumstances, that the fluid driving the eruption was either partially non-magmatic or had cooled below magmatic temperature. The model results and observations also suggest that atmospheric humidity boosted the height of small volcanic plumes by at least a few kilometers relative to heights that would be predicted on the basis of plume height-eruption intensity relations for larger eruptions. Lack of more accurate information on plume height and eruption intensity for this eruption prevents a more detailed analysis.

5. Discussion

[22] This model, like most models of atmospheric plumes, necessarily involves important simplifications. Its value lies less in its ability to simulate specific eruptions than in its capability of showing how plume dynamics change with variations in specific parameters. How might the height, or velocity profile, or mass fraction condensed water in a plume be affected by, say, a cold-air inversion layer? How could changes in the tropopause elevation affect the height of a plume? These questions and others have been answered in a general way by published studies; but printed works do not always explore the full range of parameters or allow the possibility for individual exploration. Graphical models like Plumeria help add this dimension.

Appendix A: Details on the Plumeria GUI and Its Use

[23] Figure 1 in the main text shows the user interface for Plumeria. On the left-hand side of the window are a series of text boxes through which users enter input parameters; atmospheric conditions in the upper left and vent properties in the middle left. For the parameters shown in the text boxes, the labels at the base of the "Vent properties" frame give the mass flow rate, mixture temperature, fraction of the total water in the mixture as vapor, and mixture sound speed. Changes in the magma temperature, gas content, percentage of water added, and vent elevation (in the atmospheric properties frame) prompt a recalculation of these properties. The mass flux value refers to the total mass flux at the vent, including magma, magmatic gas, water, and steam. The wt% gas text box refers to magmatic gas prior to mixing with water. Because the atmospheric pressure is a function of vent elevation, the boiling-point temperature at that pressure is recalculated when the vent elevation is changed. For magma-water mixtures that exit the vent at boiling-point temperatures, a change in vent elevation will result in slight changes in the mixture temperature given.

[24] Among atmospheric properties, the lapse rate text box refers to the thermal lapse rate in the troposphere; its value is negative because temperature decreases as elevation increases. The tropopause elevation text box refers to the elevation at the base of the tropopause. From the base to the top of the tropopause (whose height is the sum of the "tropopause elevation" entry plus the "tropopause thickness" entry), atmospheric temperature is assumed to be constant; the tropopause temperature is calculated from the tropospheric lapse rate and the tropopause elevation.

[25] To run the model, enter the appropriate input values in the text boxes and press the "calculate" command button in the lower left. The calculated profiles of velocity, density, plume radius, temperature, and mass fraction of liquid and ice are plotted (from left to right) in the plot areas to the right of the input text boxes. Up to five model runs can be plotted at a time, after which users must press the "clear plots" command button in the lower left before calculating more runs. Users may write output to a text file titled "outfile.txt" by clicking the "write output" radio button in the lower left. A sample of the output from one run is shown in Figure A1.

[26] The model can be obtained by downloading the zipped file linked to this article. Once the zipped file is downloaded, unzip it to a folder on your hard drive and then double-click on the icon named "setup.exe." Follow the on-screen instructions. After installation the program will be included in the Programs list on the Start button. The executable program will be under "Program files\Plumeria 2" You must be using a computer with a Microsoft Windows® operating system (or a Windows emulator), running Windows 98® or later with at least 3 megabytes storage capacity on the hard drive. Program installation requires administrative privileges; if you do not have such privileges you will need the help of a system administrator to install this program.

A1. Entering Atmospheric Data

[27] Figure A2 shows atmospheric sounding data copied from a section of a sounding by the

```
Output from Plumeria 2

Input values:
 Tropopause elevation (km):            11.0
 Height of tropopause (km):            9.0
 Thermal lapse rate (C/km):            -6.50
 Relative humidity, % :                0.0
 Air temperature at vent (C):          0.0
 Air pressure  at vent, atmospheres:   1.000
 Vent diameter (m):                    100.0
 Initial velocity (m/s):               100.0
 Magma temperature (C):                900.
 Weight fraction gas:                  0.030
 Magma specific heat, (J/kg K):        1000.0
 Magma density, (kg/m3):               2500.0
 Mass fraction water added:            0.000
 Mass flux, (kg/s):                    4.79e+06

i            z            m_l          m_i          u            r            T_mix        rho_mix      Time
i            meters                                  m/s          meters       Celsius      kg/m3        seconds
 1           0.00         0.0000       0.0000       100.0        50.0         1172.96      6.10         0.00
 2           1.00         0.0000       0.0000       99.8         50.8         1171.59      5.94         0.01
 3           2.53         0.0000       0.0000       99.4         52.0         1169.51      5.71         0.02
 4           4.67         0.0000       0.0000       99.0         53.6         1166.60      5.41         0.04
 5           7.48         0.0000       0.0000       98.4         55.6         1162.82      5.07         0.07
 6           10.98        0.0000       0.0000       97.6         58.1         1158.16      4.71         0.10
 7           15.16        0.0000       0.0000       96.8         60.9         1152.69      4.35         0.14
 8           19.97        0.0000       0.0000       95.8         64.0         1146.46      4.00         0.18

. . .

 622         13472.10     0.0000       0.0006       1.0          15903.2      185.12       .32          225.00
 623         13472.12     0.0000       0.0006       1.0          16016.9      185.12       .32          225.01
 624         13472.13     0.0000       0.0006       0.9          16131.4      185.12       .32          225.03
 625         13472.14     0.0000       0.0006       0.9          16246.7      185.12       .32          225.04
 626         13472.16     0.0000       0.0006       0.9          16362.8      185.12       .32          225.05
 627         13472.17     0.0000       0.0006       0.9          16479.8      185.12       .32          225.07
```

Figure A1. Sample output from a Plumeria model run.

National Oceanic and Atmospheric Administration (NOAA), posted on their Web site http://www.arl.noaa.gov/ready-bin/profile1a.pl. Data MUST be in the format shown in this figure in order to be read. Plumeria ignores the first four lines of the input file, which are column labels and annotations, and reads the remaining tabulated data as an unformatted sequence of numbers. Only the first four numbers in each line (pressure, elevation, temperature, and dew point, respectively) are used. These

```
PRESS HGT(MSL) TEMP DEW PT  WND DIR  WND SPD
 HPA       M      C     C       DEG     M/S
 E = Estimated Surface Height

  960.   558.E  10.9    8.5   200.4     2.0
  950.   690.   10.3    8.7   192.0     2.1
  925.   911.    8.5    7.2   197.7     3.3
  900.  1137.    6.9    5.4   218.7     4.3
  875.  1369.    5.6    3.4   227.3     5.1
  850.  1606.    5.5    1.0   238.1     7.3
  825.  1850.    5.1   -1.3   246.7     9.2
  800.  2101.    4.4   -2.7   255.2    10.2
  750.  2625.    2.0   -1.7   264.6    12.8
  700.  3180.    -.9   -7.0   271.2    16.0
  650.  3768.   -4.2   -8.6   271.6    18.9
  600.  4396.   -7.1  -13.2   268.7    19.8
  550.  5071.  -10.3  -20.5   265.2    19.5
  500.  5799.  -14.9  -25.9   260.8    18.0
  400.  7448.  -27.5  -34.1   263.1    16.6
  300.  9453.  -43.1  -47.8   290.8    24.0
  250. 10655.  -52.8  -57.6   301.2    25.7
  200. 12052.  -64.0  -69.3   302.7    24.1
  150. 13810.  -64.7  -73.9   285.1    24.9
  100. 16269.  -65.5  -83.8   268.6    23.9
```

Figure A2. Meteorological data format that can be read by Plumeria.

numbers should be separated by blank spaces. The program stops reading once it encounters the first empty line after the fourth line in the file. The data should also be stored in a plain text file with the ".txt" suffix. The data can be imported into Plumeria by going to the Options menu, then to "Add multilayered atmosphere." A message box will appear warning you that data must be in the format shown in Figure A2. After clicking "Okay," a dialog box appears from which users can select the file containing meteorological data. The data are then read and shown in a new dialog box (Figure 3 in the main text). If the data have been appropriately read, press the "Accept data" command button. The relative humidity is calculated from the dew point data, and temperature and humidity are both plotted to the right in this window. Once the dialog box is closed, these data are incorporated into the model. The text boxes for all atmospheric properties except vent elevation are then disabled or grayed out in the main program window (this is why the contents of these text boxes appear gray in Figure 1). Changes in the vent elevation will cause Plumeria to recalculate the temperature and relative humidity at the vent, and enter them into the text boxes on the main form.

[28] To return to a simple atmosphere, go to the Options menu and choose "Restore simple atmosphere." The text boxes for atmospheric properties on the main form will be re-enabled.

A2. Important Caveats

[29] An obvious question that can be quickly answered using Plumeria is "what happens to plume height when I change parameter A or B? When using Plumeria for this purpose, it is important to consider what other properties should be held constant while A or B are changed. The most logical property to hold constant is the mass flow rate of magma and gas, since plume height is commonly considered a function of mass flow rate. But if one were to change vent diameter in Plumeria while holding velocity, temperature, and gas content constant, the mass flow rate would change. Similarly, changes in eruptive temperature, gas content, velocity, and to a small extent, vent elevation all affect the mass flow rate. If you wish to study the effect of, say, exit velocity on plume height while keeping the mass flow rate constant, it would be most reasonable to change exit velocity and vent diameter simultaneously in such a way that mass flow rate remains constant, since exit velocity and jet diameter tend to be interdependent functions of vent geometry. Ensuring that simultaneous changes in these parameters result in no change in mass flux is fairly easy in Plumeria because the mass flux label in the Vent Properties frame immediately updates when these input parameters are altered. If you wish to alter magma gas content while keeping mass flow rate constant, it may be most appropriate to adjust the exit velocity so that its value, divided by the sound speed of the mixture, is roughly constant, and then make changes in jet diameter to ensure that the mass flow equals its original value. Similarly, adjustments in vent temperature should be followed by adjustments in exit velocity to maintain a constant Mach number, followed by adjustments in vent diameter. To make these adjustments easier, the sound speed is shown in the Vent Properties frame of the program window. The sound speed c is calculated as

$$c = \sqrt{\frac{K}{\rho_0}} \tag{A1}$$

where K is the adiabatic bulk modulus of the mixture and ρ_0 is the mixture density at the vent, whose formula is given in Appendix B. Because erupting mixtures are almost entirely gas by volume, K is roughly equal to the adiabatic bulk modulus of the gas, which is equal to the pressure p multiplied by the ratio γ of specific heat at constant pressure divided by the specific heat at constant volume. For H_2O vapor at $T = 100°$ to $1000°C$, $\gamma = 1.23–1.33$. Plumeria uses an approximate value of 1.25, which yields sound speeds within 3% of the values calculated using a variable γ in this pressure range.

[30] If external water is added to the mixture, the mass flux shown in the Vent Properties frame changes to include that of magma, gas, and external water. The mass flux of magma plus gas is equal to this value multiplied by one minus the mass fraction of water added to the mixture. If users are making multiple runs and changing the amount of external water in each run, they may wish to use a spreadsheet to calculate the total mass flux required for each run in order to keep mass flux of magma plus gas constant. The variables that should be altered in order to maintain a constant mass flux are the subject of some uncertainty that reflects our lack of understanding of how magma and water mix during eruptions. *Koyaguchi and Woods* [1996] adjusted the exit velocity, assuming

that the vent diameter should be held constant. An alternative approach would be to reduce exit velocity by an amount equal to the mass fraction of added water, and then increase vent diameter to maintain a constant mass flow rate of magma plus gas. The second approach assumes that magma and water thermally equilibrate under unconfined conditions in the atmosphere and that the process of equilibration causes expansion of the jet but does not change its bulk momentum.

A3. Some Useful Case Studies

[31] Some useful case studies in plume height and eruption rate are summarized by *Sparks et al.* [1997, chap. 5]. Some other well-documented eruptions include those of Mount Spurr, Alaska in 1992 [*Keith*, 1995] and the pre-climactic eruptions of Mount Pinatubo, Philippines [*Hoblitt et al.*, 1996].

A4. Model Updates

[32] Updates to the model, when available, will be posted at http://vulcan.wr.usgs.gov/Projects/Mastin. This Web page will also contain documentation of model updates and information on the various versions.

Appendix B: Constitutive Equations and Mathematical Derivations

[33] Plumeria integrates the equations of mass, momentum, and energy along a one-dimensional vertical profile. Input parameters include the vent radius (r_0), velocity (u_0), magma temperature (T_m), mass fraction of gas in the magma (n_0), and mass fraction external water (m_w^{ext}) added to the eruptive plume (see Table B1 for a list of variables). As explained in the main text, the model divides the plume into two parts: a momentum-dominated gas-thrust region which lies within a kilometer or two above the vent, and a buoyancy-dominated convective region at higher elevation. In the convective region, Plumeria follows the approach of *Woods* [1988, 1993] and *Sparks et al.* [1997] in assuming that the inward velocity (u^{amb}) of air being drawn into the plume is proportional to the plume's ascent velocity (u), with a constant of proportionality (ε) of ~0.09,

$$u^{amb} = \varepsilon u \tag{B1}$$

[34] It should be noted that u^{amb} is oriented horizontally inward toward the jet center whereas u is vertically upward. In the gas thrust region, Plumeria also follows *Woods* [1988] in using the following relationship:

$$u^{amb} = u\varepsilon\sqrt{\frac{\rho}{\rho^{amb}}} \tag{B2}$$

[35] The entrainment rate is the only adjustable empirical parameter in the model.

[36] The mass flux M at elevation z in the control volume is

$$M = \pi r^2 \rho u \tag{B3}$$

[37] Both ρ and u are functions of z. As a result of air entrainment, the change in the mass flux over an increment dz in elevation is $2\pi r\rho^{amb}u^{amb}dz$. This expression is combined with the formula for u^{amb} given in (B1) and (B2) to give the following expressions for mass conservation in the convective region:

$$\frac{dM}{dz} = \frac{d(\pi r^2 \rho u)}{dz} = 2\pi r\rho^{amb}\varepsilon u \tag{B4}$$

and the gas thrust region:

$$\frac{dM}{dz} = \frac{d(\pi r^2 \rho u)}{dz} = 2\pi r\varepsilon u\sqrt{\rho\rho^{amb}} \tag{B5}$$

[38] The gas thrust region is assumed to extend to an elevation at which the plume density is less than that of the ambient atmosphere.

[39] The momentum conservation equation below assumes that the plume ascent is driven by the density difference between the plume and the ambient atmosphere:

$$\frac{d(Mu)}{dz} = \pi r^2\left(\rho^{amb} - \rho\right)g \tag{B6}$$

[40] The following energy equation assumes that the only heat transferred into or out of the control volume is that advected by the plume itself and by entrained air.

$$\frac{dE}{dz} = \frac{d}{dz}\left[M\left(\frac{u^2}{2} + gZ + h\right)\right] = \left(gZ + h^{amb}\right)\frac{dM}{dz} \tag{B7}$$

[41] Here E is total energy flux; h and h^{amb} are the specific enthalpies (i.e., enthalpy per unit mass) of the plume mixture and of the ambient atmosphere,

Table B1. Variables

Variable	Name	Units
c	sound speed of erupting mixture	m/s
c_{pa}	specific heat of dry air at constant pressure	J/(kg K)
c_{pi}	specific heat of ice at constant pressure	J/(kg K)
c_{pl}	specific heat of liquid water at constant pressure	J/(kg K)
c_{pm}	specific heat of pyroclasts at constant pressure	J/(kg K)
c_{pv}	specific heat of water vapor at constant pressure	J/(kg K)
E	total energy flux	W
e	partial pressure of water vapor	Pa
$e_s(T)$	partial pressure of water at saturation at temperature T	Pa
g	gravitational acceleration	m/s^2
H_{trop}	tropopause thickness	m
h	specific enthalpy	J/(kg K)
h_0	enthalpy at a reference temperature T_0	J/kg
h^{amb}	specific enthalpy of ambient atmospheric air	J/kg
h_b	specific enthalpy of phase change	J/kg
h_{bl}	specific enthalpy of mixture at boiling, assuming all water is in liquid form	J/kg
h_{bv}	specific enthalpy of mixture at boiling, assuming all water is in vapor form	J/kg
h_{fl}	specific mixture enthalpy at freezing, assuming all excess water is in liquid form	J/kg
h_{fi}	specific mixture enthalpy at freezing, assuming all excess water is ice	J/kg
h_m	specific enthalpy of pyroclasts	J/kg
h_s	specific mixture enthalpy at water saturation temperature	J/kg
h_v	specific enthalpy of water vapor	J/kg
h_{vent}	enthalpy of erupting mixture at vent	J/kg
K	Bulk modulus of erupting mixture at the vent	Pa
$\mathrm{M_a}$	molar weight of dry air (0.02897 kg/mole)	kg/mole
$\mathrm{M_w}$	molar weight of water (0.0180152 kg/mole)	kg/mole
M	total mass flux in plume	kg/s
M_a	mass flux of dry air in plume	kg/s
M_m	mass flux of pyroclasts in plume	kg/s
M_w	mass flux of water in plume	kg/s
m_a	mass fraction dry air in plume	
m_a^{amb}	mass fraction dry air in ambient atmosphere	
m_i	mass fraction ice in plume	
m_l	mass fraction liquid water in plume	
m_m	mass fraction magmatic fragments in plume	
m_v	mass fraction water vapor in plume	
m_v^{amb}	mass fraction water vapor in ambient atmosphere	
m_w	mass fraction total water (all phases) in plume	
m_w^{ext}	mass fraction external water added to initial mixture	
n_0	mass fraction gas in magma	
p	pressure	Pa
p_0	reference pressure	Pa
p_w	partial pressure of water in the plume, assuming all water is in vapor form	Pa
Q	Eruption rate (dense-rock equivalent of magma	m^3 s^{-1}
R_a	gas constant for dry air	J/(kg K)
R_w	gas constant for water	J/(kg K)
r	column radius	m
r_h	relative humidity	–
r_0	vent radius	m
s	specific entropy	J/(kg K)
T	temperature	K
T_b	boiling temperature	K
T_c	critical temperature of water (647.25 K)	K
T_D	dew point temperature	K
T_m	initial magmatic temperature	K
T_0	reference temperature for enthalpy calculations	K
T_w^{ext}	Temperature of external added water (10°C)	K
u	plume ascent velocity (vertical)	m/s
u^{amb}	lateral velocity of air entering the plume	m/s
u_0	eruption velocity at vent	m/s
w	mass ratio of water vapor to air	
w_s	mass ratio of water vapor to air under saturated conditions	

Table B1. (continued)

Variable	Name	Units
Z	height of a specific point above the vent	m
z	elevation variable (positive upward)	m
α	fitting coefficient for c_p for gases	
β	fitting coefficient for c_p for gases	K^{-1}
ε	entrainment coefficient	
γ	fitting coefficient for c_p for gases	K^{-2}
δ	fitting coefficient for c_p for gases	K^{-3}
ϕ	fitting coefficient for c_p for gases	K^{-4}
ρ	plume density	kg/m^3
ρ^{amb}	density of the ambient atmosphere	kg/m^3
ρ_0	density of erupting mixture at the vent	kg/m^3
ρ_i	density of ice crystals (900 kg/m^3)	kg/m^3
ρ_l	density of liquid water (1,000 kg/m^3)	kg/m^3
ρ_m	density of pyroclasts (2,500 kg/m^3)	kg/m^3
ρ_v	density of water vapor	kg/m^3

respectively; g is gravitational acceleration, and Z is the elevation at the center of the control volume.

B1. Initial (Vent) Conditions

[42] In the absence of added external water, the mass, momentum, and energy fluxes at the vent are calculated from the exit velocity (u_0) and vent radius (r_0), which are given as input; and the mixture density (ρ_0) and enthalpy (h_{vent}), which are determined from specified values of magma temperature, gas content, and mass fraction.

Density

$$\rho_0 = \left[\frac{n_0 R_w T}{p} + \frac{(1-n_0)}{\rho_m}\right]^{-1} \tag{B8}$$

Enthalpy

$$h_{vent} = n_0 h_v(T_m) + (1-n_0)h_m(T_m) \tag{B9}$$

The terms n_0, p, R_w, T, and ρ_m are the mass fraction gas in the magma-gas mixture, pressure at the vent, the specific gas constant for water, absolute temperature, and magma density (assumed equal to 2,500 kg m^{-3}), respectively. Equation (B8) assumes that the gas phase is water vapor whose density (ρ_v) is given by the ideal gas relation $\rho_v = p/(R_w T)$; equation (B9) indicates that the total enthalpy of the mixture equals the sum of the enthalpies of the gas at magmatic temperature ($h_v(T_m)$) and tephra at magmatic temperature and p = 1 atm ($h_m(T_m)$), multiplied by their respective mass fractions. Procedures for calculating enthalpies of these components are described below.

[43] If external water is added to the erupting mixture, Plumeria assumes that the magma, gas, and water have thermally equilibrated at atmospheric pressure before rising out of the vent. The post-mixing enthalpy is therefore equal to the sum of enthalpies of the components prior to mixing [*Mastin*, 1995], which is given by

$$h_{vent} = \left(1-m_w^{ext}\right)(1-n_0)h_m(T_m) + \left(1-m_w^{ext}\right) \cdot (n_0)h_v(T_m) + m_w^{ext} h_l\left(T_w^{ext}\right) \tag{B10}$$

where T_w^{ext} is the temperature of the liquid water prior to mixing (assumed equal to 10°C except for calculations in Appendix C, where T_w^{ext} is changed to 0°C to match values used by *Koyaguchi and Woods* [1996]) and m_w^{ext} is the mass fraction of added water. (Enthalpy terms h_{vent}, h_m, h_v and h_l are per unit mass.) After mixing, the magmatic gas and external water are all assumed to constitute a single, thermally equilibrated aqueous component having a mass fraction (m_w) equal to

$$m_w = \left[\left(1-m_w^{ext}\right)n_0 + m_w^{ext}\right] \tag{B11}$$

The mass fraction water following thermal equilibration is partitioned into liquid (m_l) and vapor (m_v) forms whose sum equals m_w:

$$m_w = m_v + m_l \tag{B12}$$

To determine the values of m_l and m_v after mixing, Plumeria calculates the enthalpy (h_{bv}) that the mixture would have at the boiling temperature (T_b) if all water were converted to vapor:

$$h_{bv} = (1-m_w)h_m(T_b) + m_w h_v(T_b) \tag{B13}$$

Table B2. Fitting Coefficients Used to Calculate Partial Pressure of Water at Saturation[a]

i	a_i
1	−7.8889166
2	2.5514255
3	−6.716169
4	33.239495
5	−105.38479
6	174.35319
7	−148.39348
8	48.631602

[a] See equation (B20).

and the enthalpy (h_{bl}) at the boiling temperature if all water were in liquid form:

$$h_{bl} = (1 - m_w)h_m(T_b) + m_w h_l(T_b) \tag{B14}$$

[44] Depending on the mixture enthalpy relative to h_{bv} and h_{bl}, the composition and temperature of the erupting mixture is determined as follows:

[45] 1. If $h > h_{bv}$, all water is in vapor form ($m_v = m_w$) and the mixture temperature lies between T_b and T_m. The mixture temperature is found by iteratively adjusting T until the mixture enthalpy equals the enthalpy calculated in (B10).

[46] 2. If $h_{bv} > h > h_{bl}$, the mixture temperature lies at the boiling point, and m_l and m_v are given by

$$m_v = m_w \frac{h - h_{bl}}{h_{bv} - h_{bl}} \tag{B15}$$

$$m_l = m_w - m_v \tag{B16}$$

[47] 3. If $h < h_{bl}$, the temperature lies below the boiling point and all the water is in liquid form. At the vent, $h < h_{bl}$ only in rare cases when the mass fraction of added water is very high (e.g., $m_w^{ext} > 0.72$ for a 900°C magma containing 3 wt% gas). The temperature is adjusted until the mixture enthalpy equals that specified in (B10).

[48] Once T, m_l, and m_v are determined, the mixture density is found from the relation

$$\rho_0 = \left[\frac{m_v R_w T}{p} + \frac{m_l}{\rho_l} + \frac{m_m}{\rho_m}\right]^{-1} \tag{B17}$$

where ρ_l is the density of liquid water, assumed to be 1,000 kg m^{-3}.

B2. Water Saturation and Mass Fraction Water Vapor and Ice

[49] Plumeria calculates the partial pressure of water vapor at saturation $e_s(T)$ using the following relations:

[50] 1. For water vapor in equilibrium with ice at $T < 273.15$ K [*Bohren and Albrecht*, 1998, equation (5.71)]:

$$\ln\left(\frac{e_s(T)}{e_s(T_0)}\right) = 22.49 - \frac{6142}{T} \tag{B18}$$

[51] 2. For water vapor in equilibrium with liquid water at $T <= 314$ K [*Bohren and Albrecht*, 1998, equation (5.67); *Haar et al.*, 1984, p. 306]

$$e_s(T) = 1 \times 10^5 \cdot \exp\left(6.3573118 - \frac{8858.843}{T} + \frac{607.56335}{T^{0.6}}\right) \tag{B19}$$

[52] 3. For $314 < T < T_c$ [*Haar et al.*, 1984, p. 306]

$$e_s(T) = 2.2093 \times 10^7 \cdot \exp\left[\frac{T_c}{T}\sum_{i=1}^{8} a_i\left(1 - \frac{T}{T_c}\right)^{\frac{i+1}{2}}\right] \tag{B20}$$

where T_c is the critical temperature of water (647.25 K), a_i are fitting coefficients given in Table B2, T_0 is the reference temperature (273.15 K), and $e_s(T_0) = 611$ Pascals is the saturated partial pressure of water at T_0 [*Haar et al.*, 1984]. All temperatures above are in Kelvin. These equations give pressures in Pascals [*Bohren and Albrecht*, 1998; *Haar et al.*, 1984, p. 306]. Equations (B19) and (B20) yield partial pressures that are accurate to within 0.05% of experimentally determined values [*Haar et al.*, 1984, Figure A.5].

[53] For undersaturated air, the partial pressure of water vapor (e) is the mole fraction of water vapor among the gaseous components (water vapor and dry air):

$$e = \frac{\frac{m_w}{M_w}}{\frac{m_w}{M_w} + \frac{m_a}{M_a}} p \tag{B21}$$

Here M_w and M_a are the molar weights of water (0.0180152 kg/mole) and dry air (0.02897 kg/mole), respectively.

[54] The mass ratio of water to dry air ($w = m_v^{amb}/m_a^{amb}$) at saturation is [*Bohren and Albrecht*, 1998, equation (6.71)]:

$$w_s = \frac{R_w}{R_a}\frac{e_s(T)}{p - e_s(T)} \tag{B22}$$

Table B3. Coefficients Used to Calculate Enthalpy of Components

Coefficient	Water Vapor	Liquid Water	Magma	Air
α	4.070		1300	3.653
β	-1.108×10^{-3}			-1.337×10^{-3}
γ	4.152×10^{-6}			3.294×10^{6}
δ	-2.964×10^{-9}			-1.913×10^{-9}
ϕ	8.07×10^{-11}			2.763×10^{-11}
h_0 (J/kg)	2.5007×10^{6}	0		2.73×10^{6}
T_0 (K)	273.15	273.15	273.15	270
p_0 (Pa)	1.013×10^{5}	1.013×10^{5}	1.013×10^{5}	1.013×10^{5}

The term R_a is the gas constant for dry air (286.98 J kg^{-1} K). The value of w_s, multiplied by the relative humidity (r_h) is the approximate mass ratio of water vapor in the air (w):

$$w \approx r_h w_s \tag{B23}$$

This approximation is reasonably exact when $w_s \ll 1$, which is the case for nearly all atmospheric conditions. (This relationship is also consistent with the definition of relative humidity by the World Meteorological Organization, $r_h \equiv w/w_s$, though the classic definition of relative humidity is $r_h \equiv e/e_s$ [*Bohren and Albrecht*, 1998].) From (B23), we can obtain the mass fraction of water vapor and dry air in the ambient atmosphere:

$$m_v^{amb} = \frac{w}{1+w} \tag{B24}$$

$$m_a^{amb} = 1 - m_v^{amb} \tag{B25}$$

[55] When dew point measurements from NOAA soundings are used in Plumeria, they are converted to relative humidity using the formula

$$r_h = \frac{e(T_D)}{e(T)} \tag{B26}$$

where T_D is the dew point temperature.

B3. Pressure, Density, and Enthalpy

[56] Density (ρ^{amb}) of the ambient atmosphere is calculated using the formula

$$\rho^{amb} = \left[\frac{p}{\left(m_v^{amb} R_w + m_a^{amb} R_a\right) T}\right] \tag{B27}$$

[57] The pressure (p) is calculated at a given elevation by integrating the relation

$$\frac{dp}{dz} = -\rho^{amb} g \tag{B28}$$

[58] Enthalpy is calculated from

$$h^{atm} = m_v^{atm} h_v(T) + m_a^{atm} h_a(T) \tag{B29}$$

where the enthalpies of water vapor ($h_v(T)$) and dry air ($h_a(T)$) are at the specified temperature. These components both act as ideal gases under meteoric conditions; hence their enthalpies are functions of temperature only and are given by

$$h_a = h_a(T_0) + \int_{T_0}^{T} c_{pa}(\tau) d\tau \tag{B30}$$

$$h_v = h_v(T_0) + \int_{T_0}^{T} c_{pv}(\tau) d\tau \tag{B31}$$

where T_0 is a reference temperature, T is the specified temperature and τ is a dummy variable representing temperature. The specific heats of water vapor and dry air can be approximated with the polynomial equations [*Moran and Shapiro*, 1992, Table A-15]

$$\frac{c_{pa}(T)}{R_a} = \alpha + \beta T + \gamma T^2 + \delta T^3 + \phi T^4 \tag{B32}$$

$$\frac{c_{pv}(T)}{R_w} = \alpha + \beta T + \gamma T^2 + \delta T^3 + \phi T^4 \tag{B33}$$

Values of fitting coefficients α, β, γ, δ, and ϕ are given in Table B3. The enthalpy can therefore be obtained by substituting (B32) and (B33) into (B30) and (B31), respectively, and integrating. The reference enthalpies, $h_v = 2.5007 \times 10^6$ J kg^{-1} at $T_0 = 273.15$ K and $h_a = 2.73 \times 10^6$ at $T_0 = 270$ K, are taken from *Haar et al.* [1984] and *Moran and Shapiro* [1992].

[59] The enthalpies of liquid water, ice, and magma fragments theoretically depend on both tempera-

Table B4. Enthalpies of Liquid Water at Saturation Pressure Used to Calculate h_l

T, C	h_l, J/kg
273.25	381.14
283.25	42406
293.25	84254
303.25	126090
313.25	167920
323.25	209750
333.25	251570
343.25	293430
353.25	335350
363.25	377350
373.25	419490

ture and pressure [*Moran and Shapiro*, 1992, p. 87] but the pressure contribution is negligible under atmospheric conditions and is ignored here. The enthalpy of liquid water is calculated by linear interpolation between a series of data points taken from *Haar et al.* [1984] over a range of temperatures under saturated conditions (Table B4). The enthalpies of ice and magma particles are calculated from the formulas

$$h_i = h_i(T_0) + c_{pi}(T - T_0) \tag{B34}$$

$$h_m = h_m(T_0) + c_{pm}(T - T_0) \tag{B35}$$

For ice, $T_0 = 273.15$ K, $h_i(T_0) = -333430$ J/kg, and $c_{pi} = 1850$ J kg^{-1} K^{-1}; for magma, $T_0 = 273.15$ K and $h_m(T_0) = 0$ J kg^{-1} (set arbitrarily), and $c_{pm} = 1100$ J kg^{-1} K^{-1}. *Woods* [1988] uses $c_{pm} = 1617$ J kg^{-1} K^{-1}, whereas *Koyaguchi and Woods* [1996] use $c_{pm} = 1000$ J kg^{-1} K^{-1}. The value of c_{pm} used by Plumeria was changed to agree with these other published studies during model comparisons in Appendix C.

B4. Variations in Mass Fraction Components With Elevation

[60] The mass fraction of dry air in the plume at any location is defined as

$$m_a = \frac{M_a}{M_w + M_a + M_m} = \frac{M_a}{M} \tag{B36}$$

where M_a, M_w, and M_m are the total mass fluxes of dry air, water, and solid tephra in the plume. The derivative of this term with elevation is

$$\frac{dm_a}{dz} = \frac{1}{M}\frac{dM_a}{dz} - \frac{m_a}{M}\frac{dM}{dz} \tag{B37}$$

By analogy,

$$\frac{dm_w}{dz} = \frac{1}{M}\frac{dM_w}{dz} - \frac{m_w}{M}\frac{dM}{dz} \tag{B38}$$

The expression for dm_m/dz is also analogous to (B37) except that $dM_m/dz = 0$, giving

$$\frac{dm_m}{dz} = -\frac{m_m}{M}\frac{dM}{dz} \tag{B39}$$

[61] The change in mass flux of dry air in the plume with elevation (dM_a/dz) is simply equal to the change in total mass flux (dM/dz) multiplied by the mass fraction dry air in the ambient atmosphere:

$$\frac{dM_a}{dz} = m_a^{amb}\frac{dM}{dz} \tag{B40}$$

This is also the case for dM_w/dz; though all the water in the ambient atmosphere is assumed to be in vapor form with a mass fraction (m_v^{amb}):

$$\frac{dM_w}{dz} = m_v^{amb}\frac{dM}{dz} \tag{B41}$$

[62] Substituting (B40) and (B41) into (B37) and (B38), we have

$$\frac{dm_w}{dz} = \frac{1}{M}\left(m_v^{amb} - m_w\right)\frac{dM}{dz} \tag{B42}$$

$$\frac{dm_a}{dz} = \frac{1}{M}\left(m_a^{amb} - m_a\right)\frac{dM}{dz} \tag{B43}$$

Equations (B39), (B42), and (B43) are calculated using values of M and dM/dz given in (B3) and (2) or (1), and are integrated with elevation.

[63] Velocity at a given elevation is obtained from the values of mass flux (M) and momentum flux (Mu) obtained by integrating (2) or (1) and (3):

$$u = \frac{(Mu)}{M} \tag{B44}$$

[64] Enthalpy is obtained from the total energy (E) calculated by integrating (4):

$$h = \frac{E}{M} - \frac{u^2}{2} - gZ \tag{B45}$$

[65] The temperature and mass fraction of liquid water or ice in the plume are calculated simultaneously by iteration. If all water in the plume were

in vapor form, the partial pressure of water vapor (p_w) would be

$$p_w = \frac{\frac{m_w}{\mathrm{M_w}}}{\frac{m_w}{\mathrm{M_w}} + \frac{m_a}{\mathrm{M}_a}} p \tag{B46}$$

where M_w and M_a are the molar weights of water (0.0180152 kg/mole) and dry air (0.02897 kg/mole), respectively. The pressure at a given elevation is assumed to equal that in the surrounding atmosphere. Plumeria numerically finds the temperature at which $p_w = e_s$, and then calculates the enthalpy (h_s) at this temperature assuming that $m_v = m_w$.

B5. Calculating Temperature and Mass Fraction of Hydrous Phases

[66] Under most atmospheric conditions, phase changes between liquid water and water vapor are sufficiently rapid that one can assume these phase to coexist in equilibrium. By contrast, liquid water and ice are typically not in equilibrium, with liquid water persisting in a subcooled state to temperatures well below freezing [*Bohren and Albrecht*, 1998, chap. 5; *Rogers and Yau*, 1989, chap. 6]. In eruptive plumes, volcanic ash particles provide numerous sites for ice nucleation, though it is not clear whether their number density is sufficient for ice nucleation to keep pace with the rate of cooling. Active research into ice nucleation [e.g., *Durant and Shaw*, 2005] may eventually answer this question; however for now, meteorological models account for the presence of subcooled water by simply assuming that, between −10° and −40°C, liquid water and ice coexist, and the relative proportions of these phases vary linearly within this temperature range [e.g., *Khairoutdinov and Randall*, 2003]. This relationship is adopted in Plumeria.

[67] The temperature and mass fractions of water vapor, liquid, and ice are then determined by the following procedure:

[68] 1. If $h > h_s$, the plume is undersaturated; $m_v = m_w$ and $m_l = m_i = 0$ (where m_i is the mass fraction ice). The temperature is adjusted numerically until the mixture enthalpy equals that given by (B51).

[69] 2. If $h_s > h > h_{fl}$, the plume is saturated and water is in both vapor and liquid form. Plumeria solves for T, m_l, and m_v by the following procedure:

[70] a. Make an initial guess at the temperature.

[71] b. Calculate w_s from (B28) and m_v and m_l from

$$m_v = \frac{w_s}{1 + w_s} \tag{B47}$$

$$m_l = m_w - m_v \tag{B48}$$

[72] c. Calculate the mixture enthalpy from

$$h = m_a h_a(T) + m_v h_v(T) + m_l h_l(T) + m_m h_m(T) \tag{B49}$$

[73] d. Compare the enthalpy calculated from (B49) with that from (B45). If they do not match, adjust temperature and repeat steps b and c.

[74] 3. If $h_{fl} > h > h_{fi}$, the plume is saturated at a temperature between 233.15 and 263.15 K and contains water vapor, liquid water, and ice. Guess an initial temperature based on the value of h relative to h_{fl} and h_{fi}. Calculate w_s from (B22) and m_v from (B47) for this temperature. The mass fractions of liquid and ice are then calculated from

$$m_l = (m_w - m_v)\frac{T - 233.15}{30} \tag{B50}$$

$$m_i = m_w - m_v - m_l \tag{B51}$$

Calculate enthalpy based on these mass fractions and compare it with h. If they do not match, adjust the temperature and recalculate mass fractions until the calculated enthalpy matches h.

[75] 4. If $h_{fi} > h$, then $T < 233.15$ K, the plume is saturated, and it contains water vapor and ice. The temperature and mass fractions of ice and water vapor are calculated in a procedure analogous to a through d in (2), with ice rather than liquid water as the condensed phase.

B6. Plume Density, Enthalpy, and Radius

[76] The bulk density, enthalpy, and radius of the plume are calculated from the relations

$$\rho = \left[\frac{(m_a R_a + m_v R_w)T}{p} + \frac{m_m}{\rho_m} + \frac{m_i}{\rho_i} + \frac{m_l}{\rho_l}\right]^{-1} \tag{B52}$$

$$h = m_v h_v(T) + m_a h_a(T) + m_m h_m(T) + m_l h_l(T) + m_i h_i(T) \tag{B53}$$

$$r = \sqrt{\frac{M}{\pi \rho u}} \tag{B54}$$

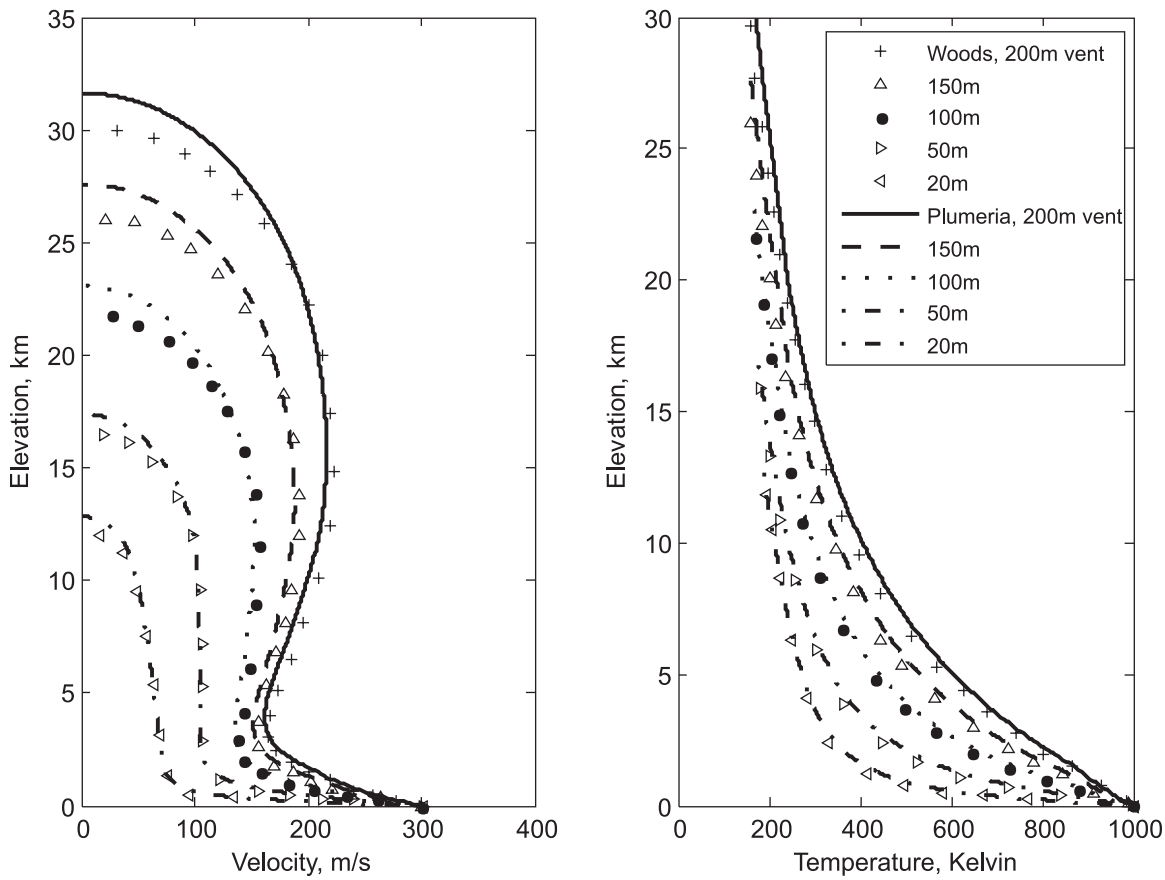

Figure C1. (left) Upward velocity and (right) temperature versus elevation for plumes exiting vents of different radii. Lines give results from Plumeria; symbols give results digitized from Figures 2a and 2b of *Woods* [1988] using the same input conditions. For these runs, u_0 = 300 m/s and the relative humidity of the atmosphere equals 0%. Other input values are listed in Table C1. It should be noted that the specific heat of magma used by Plumeria is 1100 J kg^{-1} K^{-1} but was changed to 1617 J kg^{-1} K^{-1} for these model runs to agree with the values of Woods.

where p is pressure (assumed to equal that of the ambient atmosphere at the same elevation) and ρ_i is ice density, taken as 900 kg m^{-3}. These terms are inserted back into (2) through (4) to calculate gradients for the next step.

B7. Integration

[77] Equations (2)–(4), (B28), and (B42)–(B43) are integrated using a modified form of routine rkqs.f from *Press et al.* [1992], which employs a fifth-order Runge-Kutta scheme with automatic adjustment of step size. The integration is carried out from the vent to the elevation at which the upward velocity is less than 0.1 m/s.

Appendix C: Comparison With Existing Models

[78] Figure C1 compares results from Plumeria with those from *Woods* [1988] for eruption in a dry atmosphere, using input conditions specified in Table C1. Plume heights calculated by Plumeria are a few percent higher for larger plumes and ascent rates in the convective thrust region are a percent or two less than those calculated by *Woods*

Table C1. Input Conditions Used in Model Runs Illustrated in Figures C1 and C2

Variable	Explanation	Value
H_{trop}	tropopause thickness (m)	9000
n_0	initial mass fraction gas in magma	0.03
T_m	magma temperature	1000 K
dT/dz	thermal lapse rate in troposphere (K/m)	−0.065
$(dT/dz)^{strat}$	thermal lapse rate in stratosphere (K/m)	0.0016
T_0^{amb}	atmospheric temperature at vent (K)	273
z^{trop}	Elevation of base of tropopause (m)	11000
m_w^{ext}	mass fraction water added to magma	0
z_0	vent elevation (m)	0

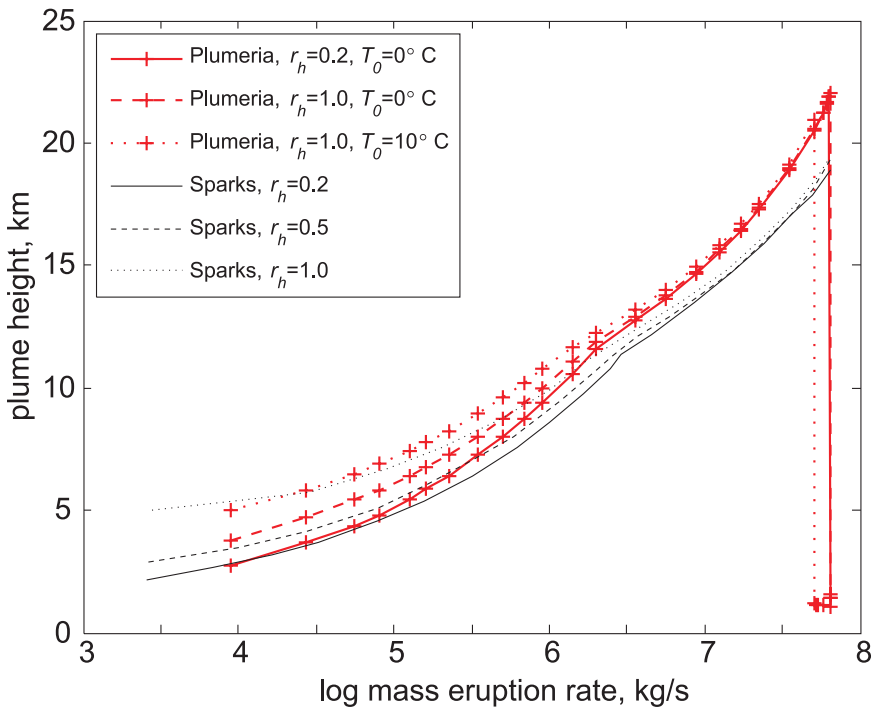

Figure C2. Comparison of volcanic plume height versus log eruption rate calculated by Plumeria with that digitized from Figure 4.11 of *Sparks et al.* [1997]. Bold red lines are results of Plumeria; fine black lines are from Sparks et al. For these runs, c_{pm} = 1100 J/(kg K), u_0 = 100 m/s, and the vent diameter was adjusted from 4 m to 340 m to give the range of mass eruption rates. Other input values are given in Table C1. All results from Plumeria assume atmospheric temperature at the vent of 0°C, except the red dotted line, which assumes atmospheric temperature at the vent equals 10°C.

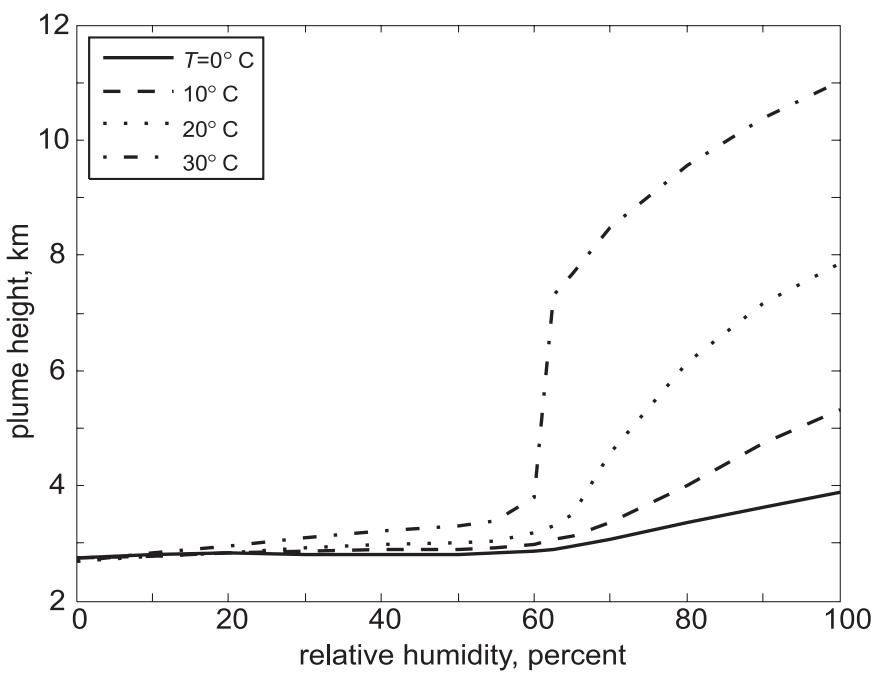

Figure C3. Variation in plume height with relative humidity for an eruption having a mass flow rate of 9×10^3 kg/s through a 4-m diameter vent. The solid, dashed, dotted, and dash-dotted lines represent atmospheric temperatures at the vent of 0°, 10°, 20°, and 30°C, respectively. For these runs, u_0 = 100 m s^{-1} and c_{pm} = 1,100 J kg^{-1} K^{-1}. All other input values are as given in Table C1.

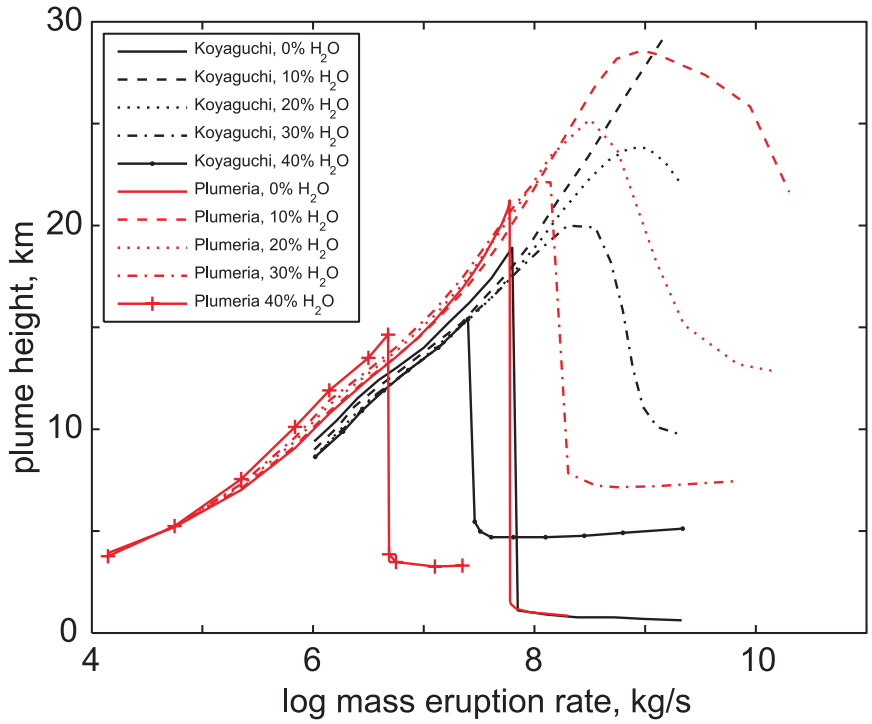

Figure C4. Eruptive plume height versus log eruption rate for a range of mass fractions water added to an eruptive plume. Red lines are Plumeria results; black lines are digitized from Figure 5 of *Koyaguchi and Woods* [1996]. Both models use relative humidity in the atmosphere of 100%, T_m = 1000 K, n_0 = 0.03, and the atmospheric conditions given in Table C1. The mass eruption rate was changed by adjusting vent diameter. As in Koyaguchi and Woods, the exit velocity of the run containing no external water is 100 m/s. For runs involving external water, the ejection velocity was increased above 100 m/s until the mass flux of magma plus gas equaled that for runs using no added water and the same vent diameter. With this adjustment, the exit velocities of runs using 10%, 20%, 30%, and 40% added water are 300, 329, 289, and 236 m/s, respectively.

[1988]. The minor discrepancies are thought to result from differences in the manner by which enthalpy is calculated and from Plumeria's consideration of condensation and ice formation.

[79] Figure C2 shows calculations of volcanic plume height versus log eruption rate calculated by Plumeria and digitized from Figure 4.11 of *Sparks et al.* [1997]. At mass flow rates exceeding $\sim 10^6$ kg/s, plume heights calculated by Plumeria are 5–10% greater than those shown in Sparks et al. At mass flow rates less than $\sim 10^5$ kg/s, Plumeria calculates a negligible effect of relative humidity on plume height, significantly less than shown by *Sparks et al.* [1997]. The effect of humidity is highly sensitive to atmospheric temperature; at a mass flow rate of $\sim 10^4$ kg/s and $r_h > 0.6$–0.7, for example, an increase in atmospheric temperature at the vent from 0°C to 20°C can double the plume height (Figure C3). In Figure C2, plume heights similar to those plotted in Figure 4.11 of *Sparks et al.* [1997, p. 97] at r_h = 1 and mass flow rates of $\sim 10^4$ kg/s are obtained by Plumeria for an atmospheric temperature at the vent of 10°C.

[80] Figure C4 shows the effect of added water on plume height as a function of mass flow rate. For this figure, the mass flow rate plotted refers only to the mass of magma plus gas, not the total mass flux including water (given in the Plumeria user page). It is important to note that exit velocities in this figure differ for different values of added external water, to ensure that the mass flux of magma plus gas is the same for a given vent diameter. The Plumeria results are qualitatively similar those in Figure 5 of *Koyaguchi and Woods* [1996], although maximum plume heights are about 10% higher and, except for the dry scenario, maximum plume heights occur at mass fluxes about a half order of magnitude lower than those of *Koyaguchi and Woods* [1996]. Plumeria predicts column collapse at somewhat lower mass eruption rates than pre-

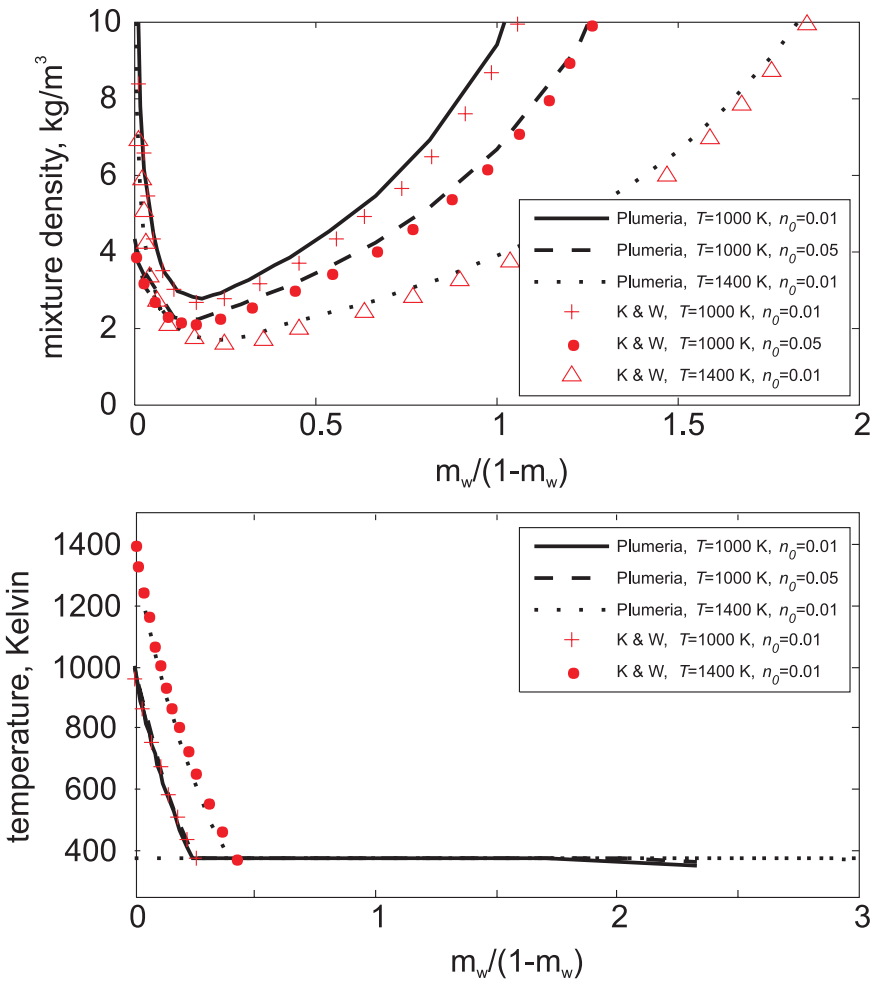

Figure C5. (top) Density and (bottom) temperature of erupting mixtures as a function of the mass ratio of water to magma plus gas exiting the vent. Initial properties of the magma are given in the legend. Solid, dashed, and dotted lines give results calculated by Plumeria. Symbols give results digitized from Figures 2b and 2c of *Koyaguchi and Woods* [1996]. The value of c_{pm} for these runs was adjusted to 1,000 J kg^{-1} K^{-1} to agree with the model of Koyaguchi and Woods.

dicted by Koyaguchi and Woods, with the discrepancy increasing as the mass fraction added water increases. At 40% added water, Plumeria predicts column collapse at about one sixth the mass eruption rate predicted by Koyaguchi and Woods.

[81] As with Figure C1, I assume that differences in plume height and column collapse threshold result from slightly different formulations for enthalpy of the various phases in the eruptive plume. A simple check of the eruptive mixture density and temperature calculated by Plumeria and *Koyaguchi and Woods* [1996] for magma-water mixtures (Figure C5) shows that both are providing roughly the same initial conditions. Slight changes in initial conditions of an erupting magma-water mixture however can lead to significant changes in the mass eruption rate at which column collapse occurs. For example, for the case of 40% added water, Plumeria calculates that, following thermal equilibration between magma and water, the temperature of the erupting mixture is 100°C and the aqueous component consists of 72% liquid and 28% vapor by mass. Changing these proportions to 71% and 29%, respectively, more than doubles the eruption-rate threshold for column collapse in Figure C4, from 8×10^6 to 1.8×10^7 kg s^{-1}. This small change in liquid-vapor proportions would be expected if the temperature of added water were increased from 0° to 10°C.

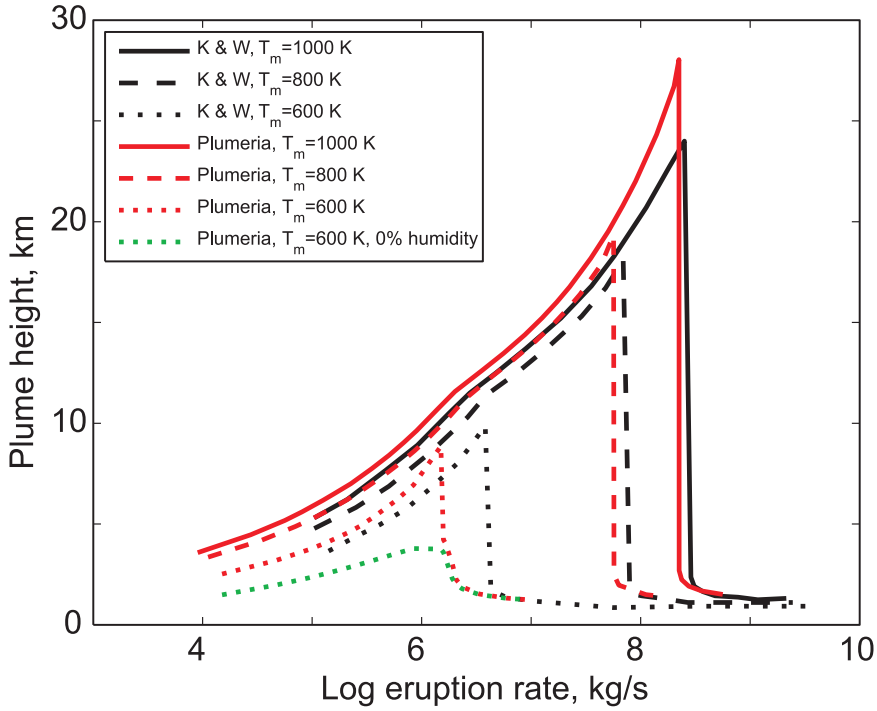

Figure C6. Comparison of plume height versus log eruption rate, with different lines representing different temperatures of the eruptive plume. Black lines were digitized from Figure 7b of *Koyaguchi and Woods* [1996]. Red lines represent Plumeria output. The green line represents Plumeria output for T = 600 K using an atmosphere containing 0% humidity (the other runs use an atmosphere containing 100% humidity). As in Figure 7 of Koyaguchi and Woods, the Plumeria runs include 1% added external water. Log eruption rate plotted here represents only the dry eruption rate without added water; runs using temperatures of 800 K and 600 K are assumed to contain a magma:lithic ratio of 1:0.5 and 1:2, respectively. Moreover, as in Koyaguchi and Woods, the ejection velocity is adjusted for each run so that the mass flux of magma + gas through a vent of a given diameter is equal to that in a dry eruption having an ejection velocity of 100 m/s.

[82] For volcanic plumes containing lithic fragments (Figure C6), relations between mass flux and plume height are similar to those of *Koyaguchi and Woods* [1996] but bear a few differences that are worth noting. At magmatic temperature (T = 1000 K), column collapse occurs at roughly the same mass flux, though the maximum column height calculated by Plumeria is about 15% higher. At lower eruption temperature, the mass flux at column collapse predicted by Plumeria is higher than that of Koyaguchi and Woods with the discrepancy increasing as temperature decreases. As in Figure C3, Figure C6 illustrates the dry mass flux (without added water). As in Koyaguchi and Woods, 1% external water with initial temperature of 0°C is added to these plumes, resulting in actual vent temperature of 963 K, 766 K, and 570 K (690°C, 493°C, and 297°C), respectively. The exit velocity was adjusted to 127 m/s so that the mass flux through a vent of a given diameter equals that of a dry eruption through the same-diameter conduit at u_0 = 100 m/s. Differences between Plumeria and the model of Koyaguchi and Woods may be related to slightly formulas for the thermal energy of air, gas, and water.

[83] The effect of water on a steady plume illustrated in Figure 5 of *Koyaguchi and Woods* [1996] may in part result from some oversimplification. The eruption velocities of the magma-water mixtures in Figure C5 suggest an increase in both the kinetic energy and the total energy of the erupting mixture. In order to conserve total energy, the kinetic increase should be offset by a decrease in plume enthalpy; this was not done in the Figure C5 plots (either for Plumeria results or those of Koyaguchi and Woods), resulting in an addition of several percent to the total energy that may have affected plume height in a minor way. More importantly, in real hydromagmatic eruptions, the partitioning of energy into kinetic and thermal forms, i.e., the "explosivity" of the mixture, depends on the mixing conditions, the degree of

confinement, and other factors. The partitioning of these two forms of energy may also affect volcanic plume height. Further studies of this issue may be a fruitful avenue of research.

Acknowledgments

[84] I wish to acknowledge the USGS Volcano Hazards Program for allowing me the time and facilities to work on this project. Tephra thicknesses and visual observations of the 8 March 2005 eruption were collected by the staff of the USGS Cascades Volcano Observatory, in particular Dave Sherrod and Jim Vallance. Observations of the tephra characteristics and their similarity to dome gouge samples were made by Carl Thornber. Interpretation of satellite imagery was provided by John Ewert and David Schneider. Suggestions on coding aspects of the model related to water condensation and ice formation were kindly provided by Peter Blossey and Chris Bretherton. Reviews by Roger Denlinger, Joseph Walder, Amanda Clarke, Lionel Wilson, and Takehiro Koyaguchi have significantly improved this paper.

References

Batchelor, G. K. (1954), Heat convection and buoyancy effects in fluids, *Q. J. R. Meteorol. Soc.*, *80*, 339–358.

Bohren, C. F., and B. A. Albrecht (1998), *Atmospheric Thermodynamics*, 402 pp., Oxford Univ. Press, New York.

Bonadonna, C., and J. C. Phillips (2003), Sedimentation from strong volcanic plumes, *J. Geophys. Res.*, *108*(B7), 2340, doi:10.1029/2002JB002034.

Carey, S., and R. S. J. Sparks (1986), Quantitative models of the fallout and dispersal of tephra from volcanic eruption columns, *Bull. Volcanol.*, *48*, 109–125.

Durant, A. J., and R. A. Shaw (2005), Evaporation freezing by contact nucleation inside-out, *Geophys. Res. Lett.*, *32*, L20814, doi:10.1029/2005GL024175.

Glaze, L. S., and S. M. Baloga (1996), Sensitivity of buoyant plume heights to ambient atmospheric conditions: Implications for volcanic eruption columns, *J. Geophys. Res.*, *101*, 1529–1540.

Haar, L., J. S. Gallagher, and G. S. Kell (1984), *NBS/NRC Steam Tables*, 320 pp., Taylor and Francis, Philadelphia, Pa.

Hinze, J. O. (1975), *Turbulence*, 790 pp., McGraw-Hill, New York.

Hoblitt, R. P., E. W. Wolfe, W. E. Scott, M. R. Couchman, J. S. Pallister, and D. Javier (1996), The Preclimactic eruptions of Mount Pinatubo, June 1991, in *Fire and Mud: Eruptions and Lahars of Mount Pinatubo, Philippines*, edited by C. G. Newhall and R. S. Punongbayan, pp. 457–511, Univ. of Wash. Press, Seattle.

Houlié, N., P. Briole, A. Nercessian, and M. Murakami (2005), Volcanic plume above Mount St. Helens detected with GPS, *Eos Trans. AGU*, *86*, 277–281.

Keith, T. E. C. (Ed.) (1995), *The 1992 Eruptions of Crater Peak Vent, Mount Spurr Volcano, Alaska*, 220 pp., U. S. Govt. Print. Off., Washington, D. C.

Khairoutdinov, M. F., and D. A. Randall (2003), Cloud resolving modeling of the ARM summer 1997 IOP: Model formulation, results, uncertainties, and sensitivities, *J. Atmos. Sci.*, *60*, 607–625.

Koyaguchi, T., and A. Woods (1996), On the formation of eruption columns following explosive mixing of magma and surface water, *J. Geophys. Res.*, *101*, 5561–5574.

Mastin, L. G. (1995), Thermodynamics of gas and steam-blast eruptions, *Bull. Volcanol.*, *57*, 85–98.

Moran, M. J., and H. N. Shapiro (1992), *Fundamentals of Engineering Thermodynamics*, 2nd ed., 804 pp., John Wiley, Hoboken, N. J.

Moran, S. C., P. J. McChesney, and J. B. Johnson (2007), Seismicity associated with explosions at Mount St. Helens during the 2004–2005 lava-dome eruption, in *A Volcano Rekindled: The Renewed Eruption of Mount St. Helens, 2004–2006*, edited by D. R. Sherrod, W. E. Scott, and P. H. Stauffer, *U.S. Geol. Surv. Prof. Pap.*, in press.

Morton, B. R., G. Taylor, and J. S. Turner (1956a), Turbulent gravitational convection from maintained and instantaneous sources, *Proc. R. Soc. London, Ser. A*, *234*, 1–23.

Morton, B. R., G. I. Taylor, and J. S. Turner (1956b), Turbulent gravitational convection from maintained and instantaneous sources, *Proc. R. Soc. London, Ser. A*, *234*, 1–23.

Pallister, J. S., M. Reagan, and K. V. Cashman (2005), A new eruptive cycle at Mount St. Helens?, *Eos Trans. AGU*, *86*, 499–500.

Press, W. H., W. T. Vetterling, S. A. Teukolsky, and B. P. Flannery (1992), *Numerical Recipes*, 2nd ed., 933 pp., Cambridge Univ. Press, New York.

Rogers, R. R., and M. K. Yau (1989), *A Short Course in Cloud Physics*, 290 pp., Elsevier, New York.

Scott, W. E., D. Sherrod, and C. A. Gardner (2007), Overview of 2004 to 2005, and continuing, eruption of Mount St. Helens, Washington, in *A Volcano Rekindled: The Renewed Eruption of Mount St. Helens, 2004–2006*, edited by D. R. Sherrod, W. E. Scott, and P. H. Stauffer, *U.S. Geol. Surv. Prof. Pap.*, in press.

Settle, M. (1978), Volcanic eruption clouds and the thermal power output of explosive eruptions, *J. Volcanol. Geotherm. Res.*, *3*, 309–324.

Sparks, R. S. J., M. I. Bursik, S. N. Carey, J. S. Gilbert, L. S. Glaze, H. Sigurdsson, and A. W. Woods (1997), *Volcanic Plumes*, 574 pp., John Wiley, Hoboken, N. J.

Thorarinsson, S. (1967), *Surtsey—The New Island in the North Atlantic*, 47 pp., Viking, New York.

Thring, M. W., and M. P. Newby (1953), Combustion length of enclosed turbulent jet flames, in *Fourth Symposium (International) on Combustion*, pp. 789–796, Williams and Wilkins, Baltimore, Md.

Turner, J. S. (1973), *Buoyancy Effects in Fluids*, 368 pp., Cambridge Univ. Press, New York.

United States Committee on Extension to the Standard Atmosphere (1976), *U.S. Standard Atmosphere, 1976*, 227 pp., Natl. Oceanic and Atmos. Admin., Washington, D. C.

Wilson, L., R. S. J. Sparks, T. C. Huang, and N. D. Watkins (1978), The control of volcanic column heights by eruption energetics and dynamics, *J. Geophys. Res.*, *83*, 1829–1836.

Woods, A., and M. Bursik (1991), Particle fallout, thermal disequilibrium and volcanic plumes, *Bull. Volcanol.*, *53*, 559–570.

Woods, A. W. (1988), The fluid dynamics and thermodynamics of eruption columns, *Bull. Volcanol.*, *50*, 169–193.

Woods, A. W. (1993), Moist convection and the injection of volcanic ash into the atmosphere, *J. Geophys. Res.*, *98*, 17,627–17,636.

Woods, A. W., and S. M. Bower (1995), The decompression of volcanic jets in a crater during explosive volcanic eruptions, *Earth Planet. Sci. Lett.*, *131*, 189–205.